

Aus dem Neurowissenschaftlichen Forschungszentrum der
Medizinischen Fakultät Charité – Universitätsmedizin Berlin

DISSERTATION

Optical induction of presynaptic plasticity using synaptoPAC

zur Erlangung des akademischen Grades

Doctor of Philosophy (PhD)

vorgelegt der Medizinischen Fakultät

Charité – Universitätsmedizin Berlin

von

Silvia Oldani

aus Magenta, Italien

Datum der Promotion: 04.03.2022

Contents

1. Abstract	i
2. Zusammenfassung	iii
3. Introduction	1
4. Materials and Methods	3
4.1 Molecular biology and viral constructs	3
4.2 Cell culture of ND7/23 cells and of autaptic granule cells	3
4.3 Immunocytochemistry and confocal microscopy	4
4.4 Electrophysiology on cultured cells	4
4.5 Stereotactic surgeries	5
4.6 Electrophysiology on acute brain slices	6
4.7 Statistics	7
5. Results	8
5.1 Construct design and validation	8
5.2 SynaptoPAC potentiates transmission in cultured granule cells	10
5.3 SynaptoPAC potentiates transmission at mossy fibres	11
5.4 SynaptoPAC does not potentiate transmission at Schaffer collateral	15
5.5 Optical and pharmacological induction in comparison	16
6. Discussion and outlook	17
7. References	20
8. Affidavit	23
9. Detailed Declaration of Contribution	24

10. ISI Web of Knowledge Journal Citation Report	26
11. Publication	30
12. Curriculum Vitae	51
13. Complete list of Publications	53
14. Acknowledgments	54

1. Abstract

A major topic in neuroscience is the cellular basis of learning and memory. Memories are stored in neuronal engrams, co-active neurons that are synaptically connected. Synaptic plasticity, due to its ability to alter synaptic weight within a neuronal network, has been hypothesised to play a role in information storage. Despite decades of research, little is known about presynaptic plasticity, a form of plasticity defined as activity-dependent modulation of neurotransmitter release. Remarkably, the specific contribution of presynaptic plasticity to behaviour is unknown, which is in part due to a lack of methods that allow its specific *in vivo* manipulation.

In order to overcome these limitations, we have engineered and characterised synaptoPAC, a novel optogenetic tool that allows induction of presynaptic plasticity. SynaptoPAC is designed as the fusion of the photoactivated adenylyl cyclase bPAC to the presynaptic vesicle protein synaptophysin. The design allows an increase of cyclic adenosine monophosphate (cAMP) in presynaptic terminals using light. Elevated presynaptic cAMP was previously demonstrated to cause an increase in release probability and induce presynaptic potentiation at specific synapses.

With immunofluorescence imaging of cultured neurons we demonstrated that synaptoPAC is enriched at presynaptic terminals, as indicated by its co-localization with the synaptic vesicle protein VGLUT1. We verified the light-driven increase of cAMP by synaptoPAC by performing electrophysiological whole-cell recordings of ND7/23 cells co-expressing synaptoPAC and the cAMP-gated channel SthK. In whole-cell recordings of autaptic hippocampal cultures expressing synaptoPAC, we observed an increase of neurotransmitter release during light stimulation as well as concomitant changes in short-term plasticity properties in granule cells, but not in other cell types. *In vivo* expression of synaptoPAC in the dentate gyrus of the hippocampus and subsequent field excitatory postsynaptic potential (fEPSP) recordings in acute brain slices enabled us to demonstrate optically induced long-term plasticity in mossy fibre-CA3 synapses. Interestingly, activation of the tool did not cause increase in the amplitude of Schaffer collateral-CA1 synapse fEPSPs in *in vitro* recordings, indicating that synaptoPAC can induce potentiation only in synapses that are already predisposed to presynaptic plasticity. Further investigations in hippocampal slice preparations of short-term plasticity in mossy fibre synapses confirmed the presynaptic nature of the optical potentiation.

Our results establish synaptoPAC as a valid tool that can be used to answer questions regarding the role of presynaptic plasticity in the brain and increase understanding of diseases characterised by impairments of this kind of plasticity.

2. Zusammenfassung

Ein wichtiges Thema der Neurowissenschaften ist die zelluläre Grundlage von Lernen und Gedächtnis. Gedächtnisspuren werden in neuronalen Engrammen gespeichert, dies sind koaktive Neurone, welche synaptisch miteinander verbunden sind. Es wird angenommen, dass synaptische Plastizität aufgrund ihrer Eigenschaft, synaptische Gewichtungen innerhalb eines neuronalen Netzwerks zu verändern, eine Rolle bei der Informationsspeicherung spielt. Trotz jahrzehntelanger Forschung ist wenig über präsynaptische Plastizität bekannt, eine Form von Plastizität, die als aktivitätsabhängige Modulation der Neurotransmitterfreisetzung definiert wird. Bemerkenswerter Weise ist kein spezifischer Beitrag der präsynaptischen Plastizität zu Verhalten bekannt, hauptsächlich auf Grund eines Mangels an Methoden, die ihre spezifische Manipulation *in vivo* erlauben.

Um diese Limitierungen zu überwinden, entwickelten und charakterisierten wir synaptoPAC, ein neues optogenetisches Werkzeug, das eine lichtvermittelte Induktion präsynaptischer Plastizität ermöglicht. SynaptoPAC wurde als Fusion der photoaktivierten Adenylylzyklase bPAC mit dem präsynaptischen Vesikelprotein Synaptophysin konzipiert. Dieses Design ermöglicht eine Erhöhung von cyclischem Adenosinmonophosphat (cAMP) in präsynaptischen Terminalen mittels Licht. Es wurde bereits gezeigt, dass erhöhtes präsynaptisches cAMP an bestimmten Synapsen eine Zunahme der Freisetzungswahrscheinlichkeit bewirkt und eine präsynaptische Potenzierung induziert.

Mittels immunfluoreszenzmikroskopischer Bildgebung von kultivierten Neuronen zeigten wir eine Anreicherung von synaptoPAC in präsynaptischen Terminalen, was durch eine Ko-Lokalisation mit dem synaptischen Vesikelprotein VGLUT1 indiziert wurde. Wir verifizierten die lichtgesteuerte Erhöhung von cAMP durch synaptoPAC mittels elektrophysiologischer Ganzzelleableitungen an ND7/23 Zellen, welche synaptoPAC und den cAMP-gesteuerten SthK Kanal koexprimierten. Bei Ganzzelleableitungen von synaptoPAC exprimierenden, autaptischen Kulturen hippocampaler Neurone beobachteten wir eine Zunahme der Transmitterfreisetzung während einer Stimulation mit Licht spezifisch in Körnerzellen, aber nicht in anderen Zelltypen, und eine damit einhergehende Veränderungen der Kurzzeitplastizität. *In vivo* Expression von synaptoPAC im Gyrus Dentatus und anschließende Feldpotenzialmessungen von exzitatorischen postsynaptischen Potenzialen in akuten Hirnschnitten ermöglichte uns, eine optisch induzierte Langzeitpotenzierung an Moosfaser-CA3 Synapsen zu demonstrieren. Interessanterweise

bewirkte die Aktivierung dieses Werkzeugs keine Verstärkung der Transmitterfreisetzung in Schaffer Kollateral-CA1 Synapsen in *in-vitro* Messungen, was darauf hindeutet, dass synaptoPAC nur in Synapsen, die bereits für präsynaptische Plastizität prädisponiert sind, eine Potenzierung induzieren kann. Weitere Untersuchungen an hippocampalen Schnittpräparationen zur Veränderung der Kurzzeitplastizität durch synaptoPAC in Moosfasern bestätigten den präsynaptischen Charakter der optischen Potenzierung.

Unsere Ergebnisse etablieren synaptoPAC als valides Werkzeug, das zur Beantwortung offener Forschungsfragen zur Rolle der präsynaptischen Plastizität im Gehirn eingesetzt werden kann, und unser Verständnis von Krankheiten verbessern könnte, welche durch eine Beeinträchtigungen dieser Art von neuronaler Plastizität gekennzeichnet sind.

3. Introduction

The brain has an incredible capacity to undergo neuroplasticity: the ability to change its properties over time. Plasticity events happen on very different temporal and spatial scales, and include rearrangements of network connections, modifications of neuronal morphology, and changes in synaptic efficacy. The first evidence that synaptic weight can increase over time was a discovery from Lømo and Bliss in 1973: using extracellular *in vivo* recordings of hippocampal granule cells (GC) in anaesthetized rabbits, they found that tetanic stimulation of the perforant path increases the synaptic input strength (Bliss and Lømo, 1973). After this first discovery, the search for a direct link between activity-dependent plasticity and memory encoding became a central enigma in neuroscience, which is still not completely solved (reviewed in Martin et al., 2000; Korte and Schmitz, 2016).

The best-characterised form of plasticity is long-term potentiation (LTP) at Schaffer collateral synapses between CA3 and CA1 pyramidal neurons. LTP induction at Schaffer collaterals typically requires the activation of postsynaptic NMDA receptors and postsynaptic Ca^{2+} influx, which results in the activation of Ca^{2+} /calmodulin dependent protein kinase (CaMKII) and subsequent insertion of additional AMPA receptors (Herring and Nicoll, 2016). In contrast to the postsynaptic modifications underlying Schaffer Collateral LTP, other synapses undergo presynaptic LTP (preLTP) with very different molecular mechanisms.

PreLTP was initially investigated at hippocampal mossy fibre (MF) and at cerebellar parallel fibre synapses (Staubli et al., 1990; Zalutsky and Nicoll, 1990; Salin et al., 1996). Induction of LTP at MF synapses is NMDA receptor independent (Harris and Cotman, 1986), and its expression results from an increase in release probability (Pr; reviewed in Schmitz et al., 2005). The enhancement of neurotransmitter release underlying MF LTP is triggered by a presynaptic signalling cascade that involves an increase in cyclic adenosine monophosphate (cAMP) (Weisskopf et al., 1994) and the subsequent activation of protein kinase A (PKA) (Huang et al., 1995). The increase in cAMP is mediated by adenylyl cyclases, in particular the Ca^{2+} /calmodulin-activated adenylyl cyclase 1 (AC1), the deletion of which impairs MF LTP (Villacres et al., 1998). MF LTP is a prototype for mechanistically similar, presynaptically expressed, NMDAR-independent and cAMP/PKA-dependent forms of LTP that are found in numerous brain regions. These regions include the cerebellum (Salin et al. 1996), thalamus (Castro-Alamancos and Calcagnotto 1999), subiculum (Wozny et al., 2008), amygdala (Lopez de

Armentia and Sah 2007), and neocortex (Chen et al. 2009). Despite decades of research in the field, the mechanisms of presynaptic plasticity and its contribution to behaviour remain elusive. This is probably due to the technical limitations of pharmacological and electrical induction of preLTP *in vivo*, which have been classically used to investigate this phenomenon, but suffer from low spatiotemporal precision. The recent development of optogenetics has facilitated research examining how neuronal assemblies can represent a memory, as well as the underlying synaptic mechanisms (Nabavi et al., 2014; Liu X et al., 2012; Ramirez et al., 2013). However, these approaches relied on the usage of channelrhodopsin-2 and its variants, which does not allow for the specific triggering cAMP-dependent presynaptic plasticity.

Our aim was to develop an optogenetic tool that would be able to optically induce presynaptic potentiation by synapse-specific modulation of Pr. To this end, we targeted a photoactivated adenylyl cyclase (PAC) to the presynapse in order to enable a light-induced increase of cAMP concentration in axonal terminals. We named this construct synaptoPAC, for synaptically-targeted photoactivated adenylyl cyclase. First, we tested its basic functionality in ND7/23 cells and its expression at presynaptic boutons. Next, we performed whole cell recordings from granule cell-enriched autaptic neuronal cultures infected with synaptoPAC to test if blue light stimulation could induce an increase in neurotransmitter release. Finally, we injected synaptoPAC in two different brain regions *in vivo* and performed *in vitro* field recordings at MF-CA3 synapses and at CA3-CA1 synapses. These experiments allowed us to investigate whether the tool is able to induce presynaptic potentiation only at synapses that display presynaptic LTP, as well as to determine under which light conditions it functions.

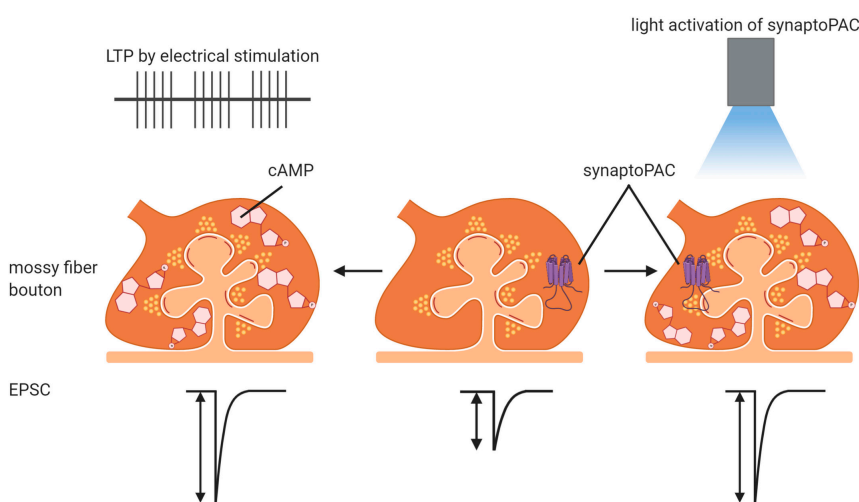


Figure 1. Schematic representation of the project idea. SynaptoPAC is expressed at presynaptic boutons and blue light stimulation enables presynaptic potentiation of synapses (right). Classically, presynaptic LTP would be induced by high-frequency train stimulation (left). Image from the editorial highlight for Oldani et al, 2020: Kees et al., 2020 (reproduced with kind permission of John Wiley & Sons, Inc.)

4. Materials and Methods

4.1 Molecular biology and viral constructs

SynaptoPAC was created as a fusion of the coding sequence of mKate2 and bPAC (Stierl et al., 2011) to the 3' end of the rat synaptophysin coding sequence by Gibson assembly (Fig.2). Synaptophysin-mKate2-bPAC, the resulting construct, was then transferred into a lentiviral expression vector under the neuron-specific human synapsin (hSyn) promoter and it was used for the characterisation of synaptoPAC's functions in cell culture experiments. For *in vivo* injections, the construct was transferred into an adeno-associated virus expression vector, and mKate2 was replaced by mScarlet, which displays higher fluorescence. AAVs were packaged as serotype 9. All viruses were provided by the Viral Core Facility of the Charité Berlin.

4.2 Cell culture of ND7/23 cells and of autaptic granule cells

ND7/23 cells (Sigma-Aldrich) were cultured in Dulbecco's Modified Eagle's Medium (DMEM; Thermo Fisher Scientific) supplemented with 10% fetal calf serum (Pan Biotech) and 0.1% penicillin/streptomycin (Thermo Fischer Scientific) at 37°C and 5% CO₂. Cells were then plated onto coverslips coated with collagen and poly-D-lysine. 24 h later, DNA encoding PAC constructs and SthK-EGFP was mixed (3:1 ratio), and then ND7/23 cells were transfected using XtremeGENE 9 reagent in a 3:1 ratio of reagent:DNA (Sigma-Aldrich). 48 h after transfection, electrophysiological recordings on transfected cells, which could be identified by their fluorescence, were performed. Cell culture of ND7/23 cells were prepared by Benjamin Rost.

To obtain granule cell enriched cultures, P0-P1 Wistar rats of either sex were decapitated, hippocampi were removed and placed in ice cold Earle's Balanced Salt Solution (EBSS; Thermo Fischer Scientific). Dentate gyri were dissected from the rest of hippocampus with a scalpel as described previously (Rost et al., 2010). Dentate gyri were enzymatically treated with 20 units per ml of papain for 45 min at 37 °C. After digestion, the enzyme solution was replaced by an inactivation solution containing albumin, trypsin inhibitor (all Thermo Fischer Scientific) and 5% fetal calf serum. Cells were isolated by manual trituration. Cells were then plated on glial cell island at density of 2.5×10^3 cells/well (35 mm well diameter) in Neurobasal-A supplemented with 2% B27 and 0.2% penicillin/streptomycin (all Thermo Fischer Scientific).

1-4 days after plating, neurons were infected with lentiviral particles encoding synaptoPAC. Neurons were incubated at 37 °C for 15-21 days before starting the experiments.

4.3 Immunocytochemistry and confocal microscopy

Cultured hippocampal neurons at DIV 15-21 were fixed with 4% paraformaldehyde in 0.1 M phosphate-buffered saline (PBS) for 10 min and then washed 3 times with PBS for 5 min. Samples were permeabilised with 0.5% Triton-X100 in PBS for 5 min and blocked for 30 min in 2% normal goat serum in 0.1% Triton-X100 in PBS. Samples were then incubated with rabbit anti-RFP (against mKate2; 1:200; Invitrogen), chicken anti-microtubule-associated protein 2 (MAP2; 1:2000; Chemicon/Merck), and guinea pig anti-vesicular glutamate transporter 1 (VGLUT1; 1:4000; Synaptic Systems) primary antibodies at room temperature for 1.5 h. Coverslips were washed 3 times with PBS before incubation with secondary antibodies conjugated with AlexaFluor-488, -555, or -647 (1:500; Invitrogen) at room temperature for 1 h. Finally, coverslips were washed 3 times with PBS and mounted with Mowiol (Carl Roth).

A TCS SP5 confocal microscope (Leica Microsystems) equipped with 63x oil immersion objective (1.4 NA) was used to image fixed neuronal cultures. Samples were illuminated using the following laser lines: 488 nm (Argon laser), 568 nm (solid state), and 633 nm (Helium, Neon). Images were acquired using the Leica Application Suite X (LAS X) software at 5x zoom, with 1024 X 1024 pixels resolution at 400 Hz, and a 16x line average for the mKate2 signal. The presynaptic enrichment of synaptoPAC was quantified using the Fiji software (Schindelin et al., 2012). For each neuron we created 4x4 pixel regions of interest (ROIs) on 20 VGLUT1-positive spots (presynaptic terminals), and 20 ROIs on MAP2-positive, but VGLUT1-negative spots (dendrites). The average intensity of the mKate2 signal in each ROI was determined, corrected for background, and the ratio between the average mKate2 signal of the VGLUT1-positive spots and the average of the MAP2-positive spots was calculated for every cell.

4.4 Electrophysiology on cultured cells

Electrophysiological recordings were performed on an IX73 inverted microscope (Olympus), coupled to a TTL-controlled LED system (pE4000, CoolLED). Fluorescent light was passed through a quadband filter set (AHF) and an 20x objective (NA 0.75; Olympus). All recordings were performed at room temperature, under safe-light illumination and in whole-cell patch clamp

configuration. Data was collected using a Multiclamp 700B amplifier under the control of a Digidata 1550 AD board and recorded in Clampex 10 (all Molecular Devices). Signals were filtered using a low-pass Bessel filter at 3 kHz, and sampled at 10 kHz. Extracellular solution contained (in mM): 140 NaCl, 2.4 KCl, 10 glucose, 10 HEPES, 2 CaCl₂, and 4 MgCl₂ (pH adjusted to 7.3 with NaOH, 300 mOsm). Borosilicate glass pipettes were filled with an intracellular solution containing (in mM): 135 K-gluconate, 17.8 HEPES, 1 EGTA, 4.6 MgCl₂, 4 Na₂-ATP, 0.3 Na-GTP, 12 disodium creatine phosphate, and 50 U/ml creatine phosphokinase, pH adjusted to 7.3 with KOH, 300 mOsm. The resistance of the electrodes ranged between 2 and 3.5 MΩ.

In recordings from ND7/23 cultures, cells co-expressing SthK-EGFP and synaptoPAC, synaptophysin-mKate2 or mKate2-bPAC were selected and voltage clamped at -60 mV. Cells were photostimulated with 474 nm light for ten ms at different intensities.

In recordings from autaptic hippocampal neuronal cultures, series resistance was compensated by 70%. Two action potential-evoked EPSCs were triggered by 1 ms somatic depolarisation from -70 to 0 mV with an interstimulus interval of 40 ms. The group II metabotropic glutamate receptor agonist L-CCG I ((2S,1'S,2'S)-2-(Carboxycyclopropyl)glycines; 10 μM; Tocris) was applied through the fast application system and used to distinguish granule cells from other glutamatergic hippocampal neurons. If application of L-CCG I reduced synaptic transmission by > 55%, neurons were classified as granule cells, if the reduction was < 40%, neurons were classified as non-granule cells. All neurons were photostimulated by 12 flashes (1 s) of 470 nm light at 0.2 Hz at 70 mW/mm². Data was analysed using AxoGraph X software (Axograph). EPSC potentiation and paired-pulse ratio changes were calculated from averaged EPSCs during baseline and light stimulation.

4.5 Stereotactic surgeries

Wild type C57BL/6N mice (P25–P31) of both sexes were anaesthetised under isoflurane (1.5% vol/vol in oxygen) during surgery and body temperature was maintained at 37°C. For analgesia animals received one subcutaneous injection of Carprofen (5 mg/kg) at the beginning of the surgery and one the end. Injections aimed to the DG (relative to bregma: anteroposterior (AP): 1.93 mm, mediolateral (ML): ±1.5 mm, dorsoventral (DV): -2.0) and to the CA3 (relative to bregma: AP: 1.75 mm, ML: 2.00 mm, DV: -2.1). 200 nl of AAV9.hSyn:synaptophysin-mScarlet-

bpAC at a rate of 40 nl/min were injected using a NanoFil syringe with a 34-gauge needle (with UMP3 microinjection system and Micro4 controller; all from World Precision Instruments). After the injection the needle remained in the targeted area for another 5 min before being withdrawn. After injection, animals recovered for at least 3 weeks before experiments to allow proper expression of the construct.

4.6 Electrophysiology on acute brain slices

Acute brain slice preparation and electrophysiological recordings were performed under continuous safelight illumination. P46-P52 WT (C57BL/6N) mice were anaesthetised using isoflurane and decapitated. Brains were transferred to ice-cold sucrose-based artificial cerebrospinal fluid (sACSF) containing (in mM): 50 NaCl, 25 NaHCO₃, 10 glucose, 2.5 KCl, 7 MgCl₂, 1 NaH₂PO₄, 0.5 CaCl₂, and 150 sucrose, saturated with 95% O₂ and 5% CO₂. Sagittal slices 300 µm thick were cut using a vibratome (Leica VT 1200S, Leica Microsystems) and incubated in sACSF at 35°C for 30 min. Slices were next incubated in ACSF solution containing (in mM): 119 NaCl, 26 NaHCO₃, 10 glucose, 2.5 KCl, 1.3 MgCl₂, 1 NaH₂PO₄, and 2.5 CaCl₂, saturated with 95% O₂ and 5% CO₂ and allowed to recover for at least 30 min at room temperature before starting electrophysiological recordings.

Recordings were performed in a submerged chamber continuously perfused with ACSF at room temperature (21–24°C), using a Multiclamp 700B amplifier (Molecular Devices). Signals were filtered at 3 kHz, sampled at 10 kHz and digitised using a Digidata 1550A AD board (Molecular Devices) or BNC-2090 interface board with PCI 6035E A/D board (National Instruments). Clampex 10.0 (Molecular Devices) or IGOR Pro 6.12 (WaveMetrics) were used as recording softwares. Optical potentiation was induced by blue light from a 470 nm LED (pE300, CoolLED), which was delivered through a 474/23 nm filter (AHF) and via a 40x (NA 0.8) water immersion objective (Olympus).

MF-CA3 synapses were stimulated at 0.05 Hz with a low-resistance glass electrode from borosilicate glass capillaries (Hilgenberg), filled with ACSF and placed in the dentate gyrus close to internal side of granule cells layers. A second low-resistance recording electrode also filled with ACSF was placed in *stratum lucidum* of area CA3, together with the objective for light stimulation. MF fEPSPs were identified by the pronounced facilitation observed upon 1 Hz stimulation and upon paired pulse stimulation at 25 Hz before photostimulation. Only fEPSP

signals that were inhibited > 80% by application of the type II metabotropic glutamate receptor agonist DCG IV ((2S,2'R,3'R)-2-(2',3'-dicarboxycyclopropyl glycine; 1 μ M, Tocris) at the end of the recording were considered to be generated by MF stimulation.

Recordings from CA3-CA1 synapses were performed by stimulation at 0.05 Hz of Schaffer collaterals with a ACSF filled glass electrode placed in *stratum radiatum* proximal to the CA3. A second ACSF filled recording electrode and the objective were placed in the *stratum radiatum* of CA1. 30 min after Schaffer collateral optical stimulation, LTP was electrically induced by four high frequency trains (100 pulses at 100 Hz, 10 s inter train interval). Only experiments in which we recorded >10% increase of the fEPSP 20-30 min after tetanic stimulation were included in the analysis. The magnitude of the presynaptic fibre volley was continuously monitored, and recordings in which the fibre volley changed >10% were discarded. Recordings were analysed using Clampfit (Molecular Devices), IGOR Pro, or Axograph X.

4.7 Statistics

Statistical analyses were performed with GraphPad Prism 5.0 and 6.0 (Graphpad Software). The D'Agostino-Pearson test was used to assess the normality of the data. No test for outliers was conducted. The number of independent cell culture preparations or number of animals is given as N, while n indicates the number of cells recorded in cultures or number of slices in fEPSP recordings. Data is expressed as means \pm SD.

5. Results

5.1 Construct design and validation

The initial discovery and description of bPAC, a photoactivatable adenylyl cyclase (PAC) from the sea bacterium *Beggiatoa*, served as inspiration for the design of synaptoPAC (Stierl et al., 2011). bPAC is a small 350 amino acid protein comprised of a light sensor that is linked to a type III adenylyl cyclase. The sensor is termed BLUF domain (blue light receptor using FAD), as it uses flavin adenine dinucleotide as a chromophore and is specifically activated with <500 nm light. Compared to the previously described euPAC (Iseki et al., 2002), bPAC has a smaller size, lower dark activity and shows stronger activation by light (Stierl et al. 2011). Since presynaptic LTP is caused by an increase of cAMP concentration at the synaptic bouton, our strategy was to fuse the presynaptic protein synaptophysin to bPAC. The red fluorophore mKate2 was added between synaptophysin and bPAC (Fig. 2). Since mKate2 can be excited by light at wavelengths longer than those utilized to activate the photosensitive adenylyl cyclase (> 500 nm; Shcherbo et al., 2009), visualisation of the construct without the concomitant activation of bPAC is possible.

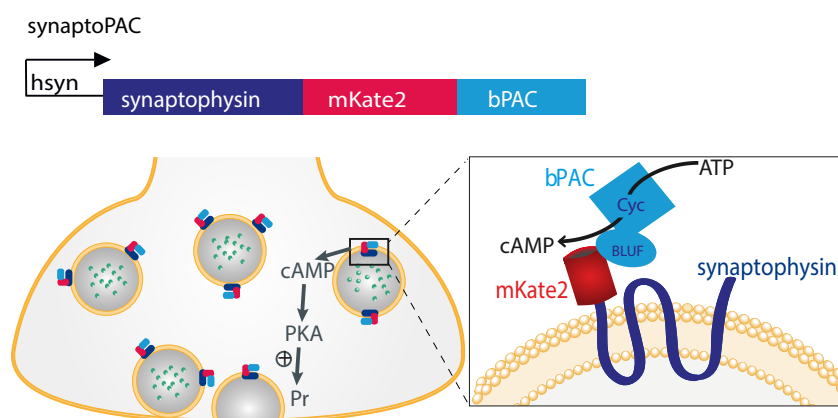


Figure 2. Illustration of the presynaptic targeting strategy for bPAC. SynaptoPAC encompasses bPAC (light blue), the fluorophore mKate2 (red) and the presynaptic protein synaptophysin (blue) and is targeted to presynaptic boutons. hsyn: human synapsin promoter; BLUF: blue light sensor using flavin adenine dinucleotide; Cyc: adenylyl cyclase domain. Figure modified from Oldani et al., 2020.

We first tested whether fusion of synaptophysin to bPAC does in fact result in enrichment of synaptoPAC at the presynaptic site. We expressed synaptoPAC or mKate2-bPAC, which is the non-targeted version of bPAC, in primary cultured neurons using lentiviral vectors. These cultures were immunostained for mKate2 to amplify its fluorescence, for the presynaptic protein VGLUT1 as synaptic marker, and for the microtubule-associated protein MAP2 as a dendritic marker. Co-staining of mKate2 with VGLUT1 showed a high expression of synaptoPAC in synapses, whereas mKate2-bPAC was expressed more diffusely (Fig. 3A,B).

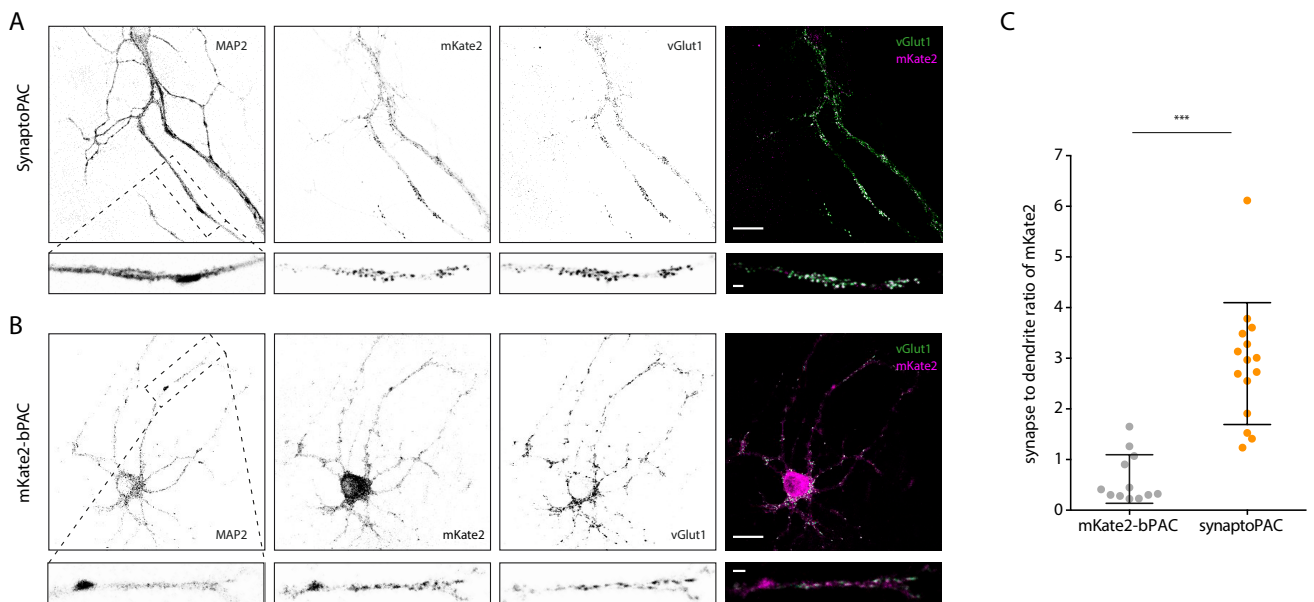


Figure 3. SynaptoPAC expression profile and quantification in cultured neurons. (A) Example images of cultured neurons expressing synaptoPAC immunostained for MAP2 (dendrites), mKate2 (synaptoPAC), and VGLUT1 (glutamatergic presynaptic terminals). Close-up of a dendrite reveals a signal overlap (white in merge) of mKate2 (magenta) and VGLUT1 (green). MAP2 is not shown in the merge. (B) Example images of cultured neurons expressing mKate2-bPAC. Scale bars for A and B: 20 μm and 2 μm for the close-up. (C) The average synapse to dendrite ratio of the mKate2 signal in cultured neurons expressing synaptoPAC and mKate2-bPAC (synaptoPAC: 2.9 ± 1.2 , $n = 15$; $N = 3$; mKate2-bPAC: 0.6 ± 0.5 , $n = 12$; $N = 3$; $p < 0.0001$, Mann Whitney U test). Figure modified from Oldani et al., 2020.

We estimated the level of synaptoPAC enrichment at presynaptic terminals compared to the non-targeted construct. mKate2 fluorescence intensity was measured within VGLUT1 positive areas (presynaptic terminals) and compared to the VGLUT1-negative, but MAP2-positive areas (dendrites). For each neuron, we then calculated the synapse to dendrite ratio of the mean fluorescence signal (for details see in Material and Methods). We found that the level of mKate2 fluorescence in presynaptic terminals was 4.8 times higher in cells infected with synaptoPAC (2.9 ± 1.2) compared to the non-targeted version, mKate2-bPAC (0.6 ± 0.5 ; Fig. 3C). This experiment showed that the targeting strategy was successful in enriching synaptoPAC in synapses. Subsequently, we wanted to verify that synaptoPAC is able to produce cAMP upon light stimulation. To address this question, we expressed synaptoPAC in ND7/23 cells together with SthK-EGFP (Fig. 4A). SthK is a potassium channel that opens upon cAMP binding to its cyclic nucleotide binding domain (Brams et al. 2014). In cells expressing both synaptoPAC and SthK, activation of synaptoPAC with blue light (474 nm, 10 ms) induced outward currents that were modulated by light intensity (Fig. 4B and C). Similar results were obtained when cells were transfected with mKate2-bPAC, however no photocurrent was found in control recordings when

synaptophysin-mKate2 was expressed (Fig. 4B and C). Experiments on ND7/23 cells were performed and analysed by Benjamin Rost.

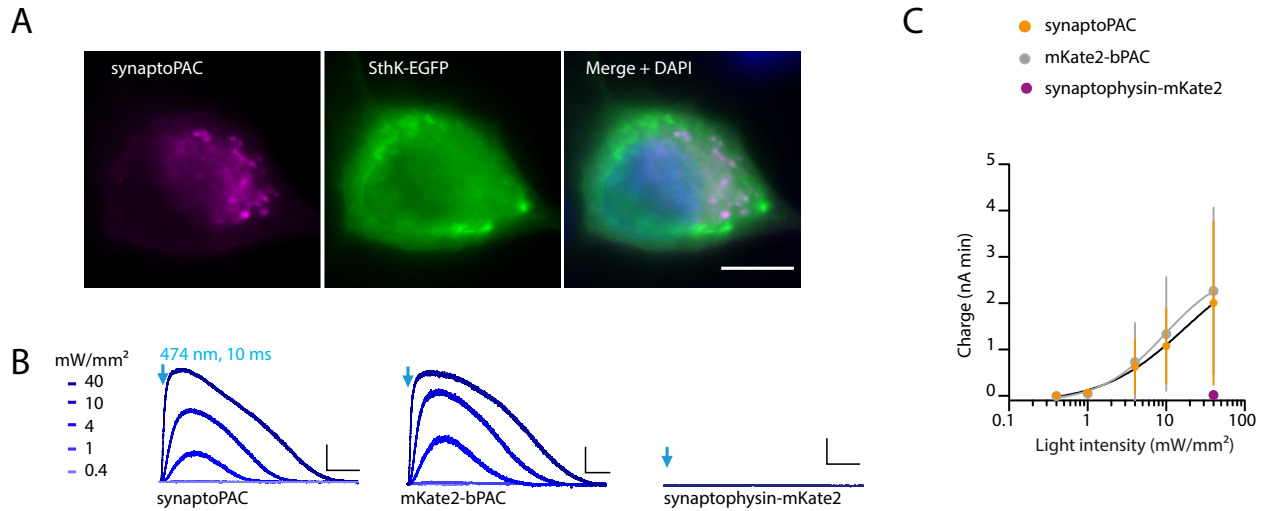


Figure 4. Verification of functional adenylyl cyclase activity of synaptoPAC (A) Fluorescence images of an ND7/23 cell expressing synaptoPAC (magenta) and SthK-EGFP (green). Scale bar: 10 μ m. (B) Representative traces of intensity-dependent outward currents in ND7/23 cells, triggered by 10 ms flashes of 474 nm light. Scale bars: 200 pA, 20 s. (C) Plot of charge (nA min) recorded at different light intensities in cells co-expressing the cAMP-gated SthK channel together with synaptoPAC (n = 8, N = 2), untargeted bPAC (n = 8, N = 2) and synaptophysin-mKate2 and SthK (n = 8, N = 2). Figure modified from Oldani et al., 2020.

5.2 SynaptoPAC potentiates transmission in cultured granule cells

In order to determine whether synaptoPAC is able to potentiate neurotransmitter release, we expressed the construct in autaptic cultures of hippocampal granule cells. During electrophysiological recordings, hippocampal granule cells were identified by application of the group II metabotropic glutamate receptor agonist L-CGG I (10 μ M; Fig. 5A). We classified neurons as granule cells (GCs) if L-CCG I reduced their transmission by >55%, and as non-granule cells (non-GCs), if they showed <40% reduction of the EPSC. Other neurons (open circle) were not included in further analysis. Optical stimulation (474 nm, 70 mW \cdot mm⁻², 12 x 1 s at 0.2 Hz) increased synaptic transmission in granule cells by 131 \pm 19%, but had no effect on transmission in non-granule cells (Fig. 5B). It is very interesting to notice that this effect is cell-type specific. Since synaptoPAC is acting via a presynaptic mechanism and is supposed to increase Pr, we expected to see an effect on short-term plasticity. For this reason, we calculated the paired pulse ratio (PPR) of EPSC amplitudes before and during blue light exposure. Results displayed in Fig. 5C support our predictions, showing a significant reduction in PPR during photostimulation in GCs but not in non-GCs.

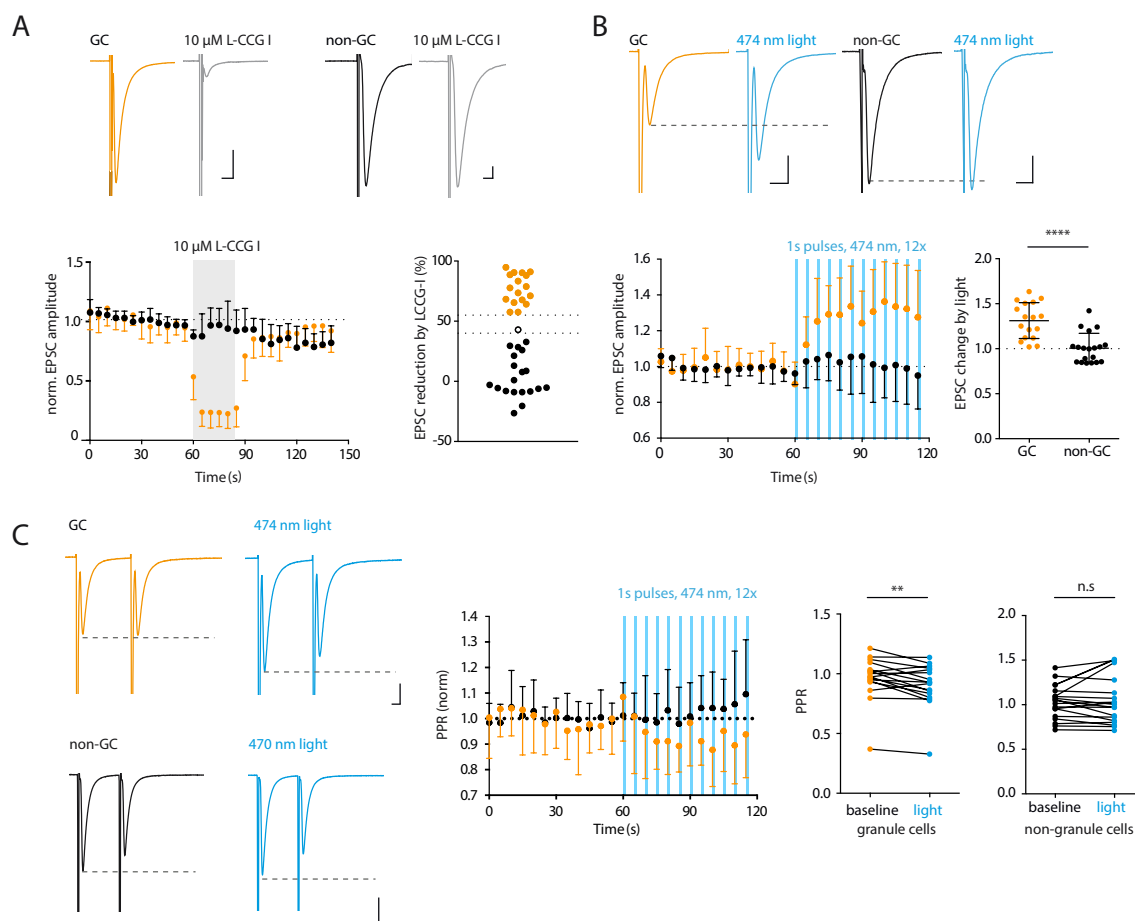


Figure 5. SynptoPAC validation in autaptic granule cells cultures. (A) Top: example traces illustrating the effect of L-CCG I on GCs and non-GCs. Scale bars, 10 ms, 1 nA. Bottom: L-CCG I effect on EPSC amplitudes for GCs (orange; $n = 17$, $N = 4$) and non-GCs (black; $n = 19$, $N = 5$) over time, and cell-type classification according to EPSC reduction by L-CCG I. (B) Top: EPSCs recorded before and after synptoPAC activation from a GC and non-GC. Scale bars: 10 ms, 1 nA. Bottom: effect of light activation of synptoPAC on EPSC amplitudes in GCs (orange; 1.31 ± 0.19 orange; $n = 17$, $N = 4$) and non-GCs (black; 1.00 ± 0.16 , $n = 19$, $N = 5$; $p < 0.0001$; unpaired t-test). (C) Paired EPSCs evoked at 25 Hz in a GC (orange) and a non-GC (black). Scale bars: 1 nA, 10 ms. Effect of light stimulation on paired-pulse ratio in GCs (baseline: 0.96 ± 0.18 , light: 0.90 ± 0.18 ; $n = 17$, $N = 4$; $p = 0.005$; Wilcoxon test) and on non-GC (baseline: 1.03 ± 0.18 , light: 1.06 ± 0.27 ; $n = 19$, $N = 5$; $p = 0.5$, paired t-test). Figure modified from Oldani et al., 2020.

5.3 SynptoPAC potentiates transmission at mossy fibres

Although our experiments in cultured neurons already provided useful insights into the potential of synptoPAC as an optogenetic tool, we reasoned that its efficacy should be tested in a more complex system, in which presynaptic LTP is traditionally investigated. For this reason, we chose to inject AAVs encoding synptoPAC into the dentate gyrus of wild type mice. Since the mKate2 incorporated into synptoPAC showed only dim fluorescence in cultures, we chose to replace it with mScarlet, a brighter fluorophore that can be excited using similar wavelength as mKate2

(Bindels et al., 2017). After 3-4 weeks, we prepared acute hippocampal sagittal slices, in which we verified successful expression of the construct in mossy fibres (MFs) by its red fluorescence (Fig. 6A). MFs were electrically stimulated and fEPSPs were recorded in CA3. After obtaining a stable baseline, optical potentiation was induced through a 40x objective placed in CA3 *stratum lucidum* close to the recording electrode (Fig. 6B).

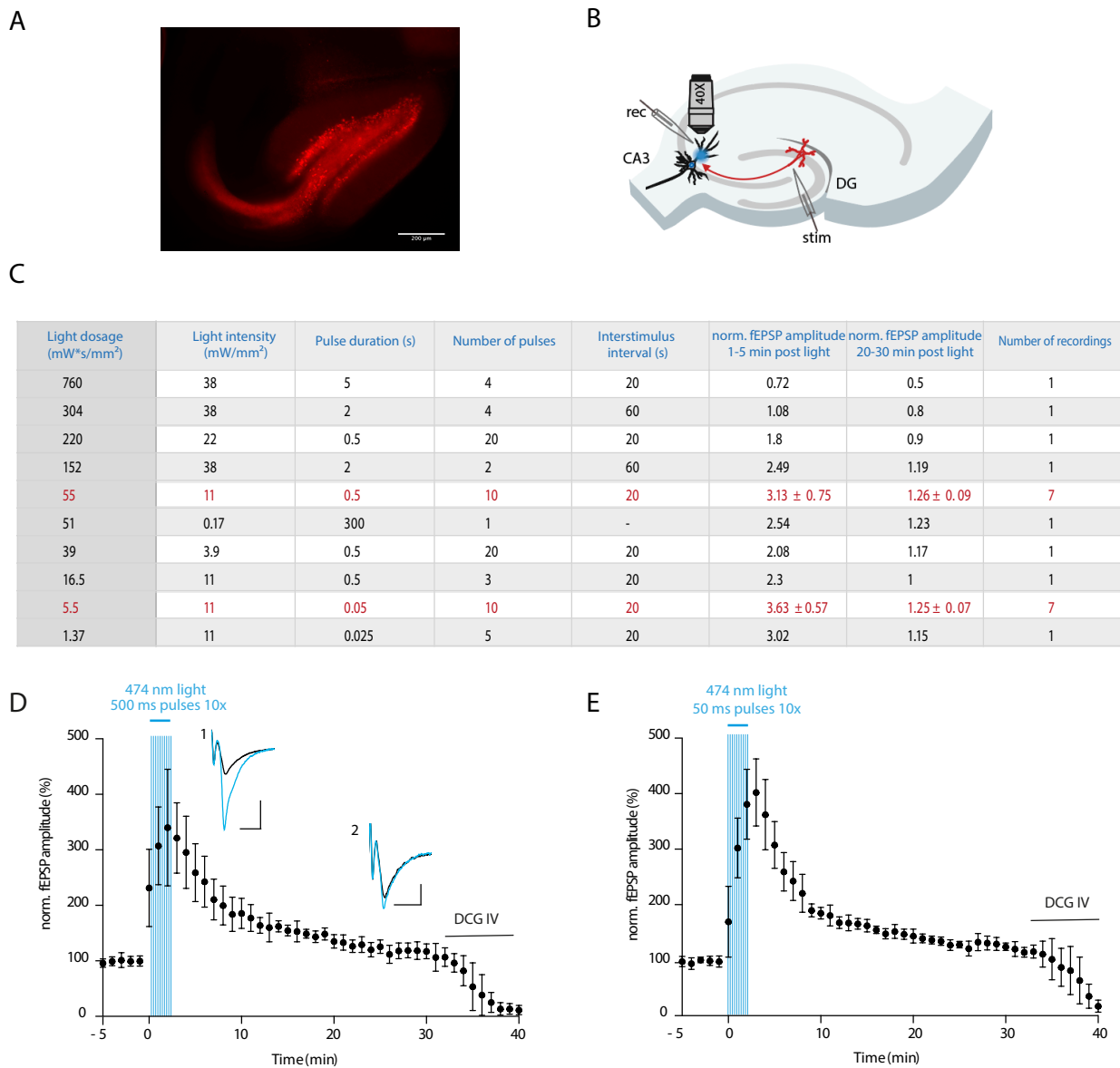


Figure 6. Optical potentiation induced at MF-CA3 synapse and tested light protocols in acute hippocampal slices. (A) Infection of dentate gyrus with AAV-synaptoPAC-mScarlet and its expression at MFs. Scale bar, 200 μ m. (B) Scheme of the experimental setup for recordings at MF-CA3 synapses, with optical stimulation in *stratum lucidum* in CA3. (C) Overview table on different photostimulation protocols used for synaptoPAC activation in MF fEPSP recordings. (D) Time course of MF fEPSPs optically potentiated with 500 ms pulses of 474 nm light repeated ten times at 0.05 Hz with 11 mW \cdot mm⁻². Example traces showing baseline synaptic transmission (black), (1) potentiated transmission in the first 5 min after illumination (blue; scale bar, 200 μ V, 20 ms), and (2) LTP after 20-30 min (scale bar: 100 μ V, 20 ms). n = 7 slices, 6 mice. (E) Time course of MF-fEPSP recordings with ten 50-ms pulses of 470 nm light at 11 mW \cdot mm⁻². This protocol results in 10x less light compared to the protocol used in

Figure 6D. $n = 7$ slices, $N = 4$ mice. Data points shown are binned to 1 min. Figure modified from Oldani et al., 2020.

A first initial exploratory phase in this set of experiments was necessary in order to figure out the light conditions under which synaptoPAC would reliably induce potentiation. For this purpose, we tested different protocols in which 474 nm light pulses were applied under different conditions: light intensity, pulse duration, repetitions of pulses, and interstimulus interval were varied and the effect of each on the optical potentiation of fEPSPs was determined (Fig. 6C). Of several light protocols tested, we ultimately chose two for repetitive testing, and found that they reliably potentiated MF fEPSPs (highlighted in red in Fig. 6C). The first protocol consisted of ten light pulses at $11 \text{ mW}\cdot\text{mm}^{-2}$, applied at 0.05 Hz, with 0.5 s pulse duration, for a total light dosage of $55 \text{ mW}\cdot\text{s}\cdot\text{mm}^{-2}$. We observed that MF fEPSP amplitudes increase to $313 \pm 75\%$ within 5 min after the light induction, and then MF fEPSP amplitudes decreased, but were still potentiated ($126 \pm 9\%$) 20 to 30 min post induction (Fig. 6D). In the second protocol we chose to reduce the duration of pulses by 10x. Despite the light dosage being 10x lower ($5.5 \text{ mW}\cdot\text{s}\cdot\text{mm}^{-2}$) than in the previous version, this protocol was equally effective for stimulating synaptic potentiation (Fig. 6E; post-light potentiation: $363 \pm 57\%$; potentiation after 20 – 30 min: $130 \pm 6.5\%$).

We predicted that the observed effect is due to an alteration of the presynaptic release probability at the MF-CA3 synapses. To confirm this hypothesis, we recorded from DG synaptoPAC-expressing slices. We measured short-term plasticity facilitation before and after optical induction of potentiation. More specifically, 5 pulses at 25 Hz and 20 pulses at 1 Hz were applied 5 min and 10 min after photostimulation, respectively, and compared to baseline values (Fig. 7A). In the 25 Hz burst, synaptoPAC-induced potentiation caused a significant decrease of the paired-pulse ratio between the second and first pulse (baseline: 2.54 ± 0.7 , post light: 1.76 ± 0.43 ; $n = 7$ slices, 6 mice; $p = 0.02$, Wilcoxon signed rank test) and also between the fifth and first pulse (baseline: 3.50 ± 1.05 , post light: 2.08 ± 1.26 ; $p = 0.02$, Wilcoxon signed rank test; Fig. 7B). In addition to this, we observed a significant decrease of 1 Hz facilitation after light compared to baseline (Fig. 7C; baseline: 4.40 ± 2.29 , post light: 2.80 ± 1.64 ; $n = 7$ slices, 6 mice; $p = 0.03$, Wilcoxon signed rank test). As control, short-term plasticity was measured in slices from animals that did not express synaptoPAC: here, we could not detect any decrease in pulse ratio (Fig. 7D) nor in 1 Hz frequency facilitation (Fig. 7E), in contrast to the significant decrease observed in recordings from synaptoPAC-expressing MFs.

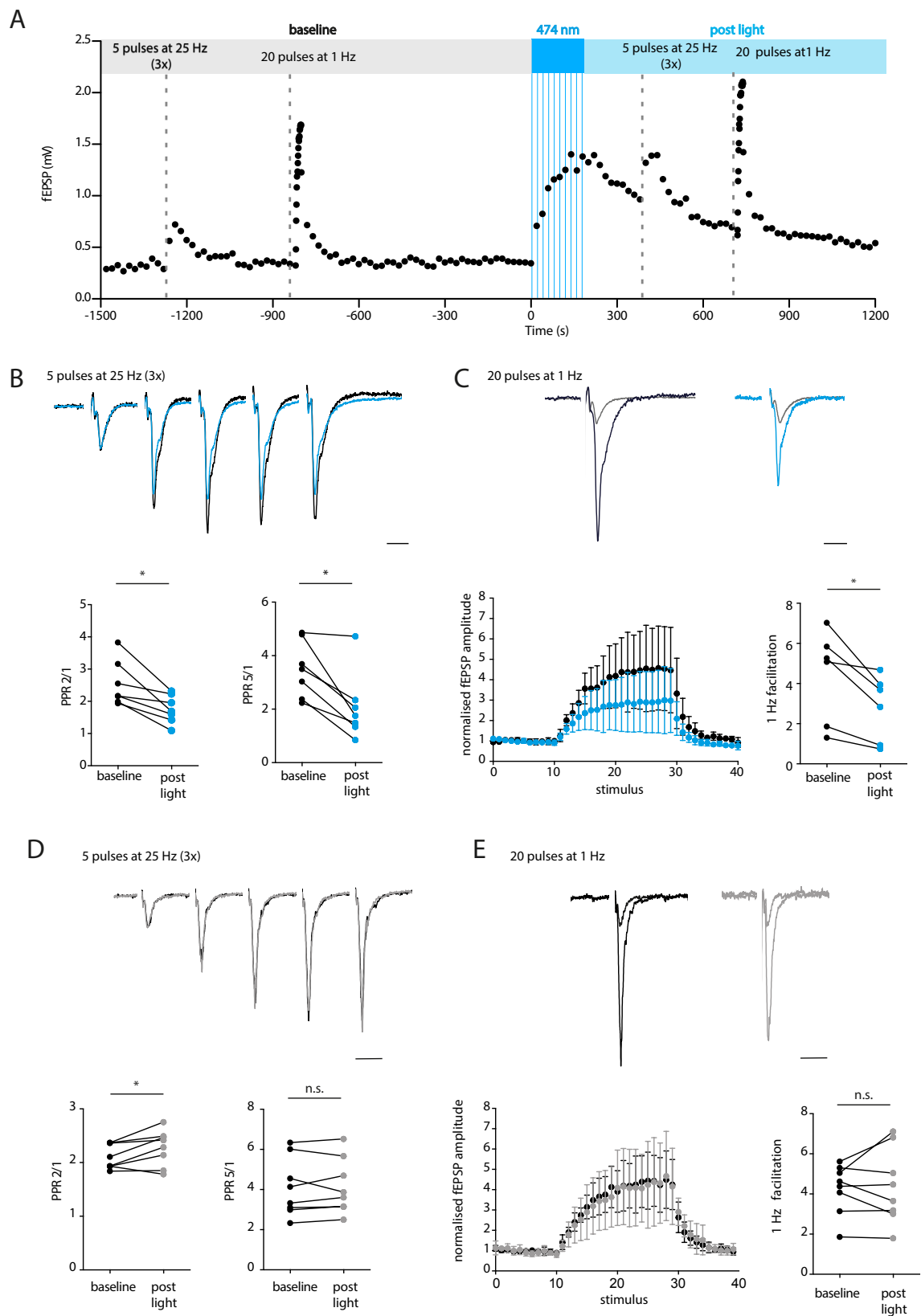


Figure 7. Decrease in short-term plasticity after synaptoPAC-induced potentiation in MF-CA3 synapses. (A) Time course of a representative experiment: MFs were first stimulated electrically with five pulses at 25 Hz and with 20 pulses at 1 Hz. SynaptoPAC was then activated by ten pulses of 474 nm light (500 ms, 11 mW·mm⁻², 0.2 Hz), and the 25 Hz and 1 Hz stimulus trains were applied again 5 and 10 min after optical induction, respectively. (B) Top: representative traces of MF fEPSPs stimulated by five pulses at 25 Hz before (black) and after light stimulation (blue). Amplitudes are scaled to the first fEPSP. Scale bar: 20 ms. Bottom: Paired-pulse ratio of the second to the first fEPSP (PPR 2/1) and the fifth to the first fEPSP (PPR 5/1) before and after light. (C) Top: traces of the first (grey) and last MF fEPSP evoked by a train of 20 stimuli at 1 Hz before (black) and after (blue) light. Bottom: Normalised fEPSP amplitude and 1 Hz facilitation before and after light.

synaptoPAC activation, scaled to the first fEPSP in the train. Scale bar: 20 ms. Bottom: 1 Hz facilitation values before (black) and after light (blue). **(D)** Top: Representative traces of paired pulse MF fEPSP before (black) and after light stimulation (grey), scaled to the amplitude of the first fEPSP, from animals not expressing synaptoPAC. Scale bar: 20 ms. Bottom: Paired-pulse ratio between the second and the first fEPSPs was significantly increased after light stimulation (baseline: 2.11 ± 0.22 , post light: 2.27 ± 0.33 ; $n=8$ slices, $N=4$ mice; $p=0.04$, paired t-test) and no significant difference was detected in paired-pulse ratio between the fifth and first fEPSPs after light (baseline: 4.10 ± 1.46 , post light: 4.15 ± 1.38 ; $p=0.73$, paired t-test). **(E)** Top: Traces showing the first and last MF fEPSP evoked by a train of 20 stimuli applied at 1 Hz before (black) and after (grey) light illumination in control animals. Traces are normalised to the first fEPSP in baseline. Scale bar: 20 ms. Bottom: 1 Hz facilitation did not change after light stimulation in absence of synaptoPAC (baseline: 4.26 ± 1.24 , post light: 4.38 ± 1.87 ; $n=8$ slices, $N=4$ mice; $p=0.73$, paired t-test). Figure modified from Oldani et al., 2020.

These results provided evidence that blue light stimulation, in the absence of synaptoPAC, does not affect neurotransmission. Taken together, these results suggest that the synaptoPAC-evoked increase in synaptic strength occurs presynaptically at the MF pathway, and corroborates the findings of previous investigations on presynaptic MF LTP (Staubli et al. 1990, Zalutsky and Nicoll 1990).

5.4 SynaptoPAC does not potentiate transmission at Schaffer collateral

Next, we investigated whether the expression of synaptoPAC could cause presynaptic potentiation in synapses that normally do not display this type of plasticity. Therefore, we *in vivo* injected wild type mice with synaptoPAC in the CA3 region and recorded in CA1 in acute slices (Fig. 8A and B). Blue light stimulation of Schaffer collaterals (500 ms pulses, $11 \text{ mW}\cdot\text{mm}^{-2}$, 10 times at 0.05 Hz, total light dosage: $55 \text{ mW}\cdot\text{s}\cdot\text{mm}^{-2}$) did not cause a significant increase in fEPSP amplitude (Fig. 8C).

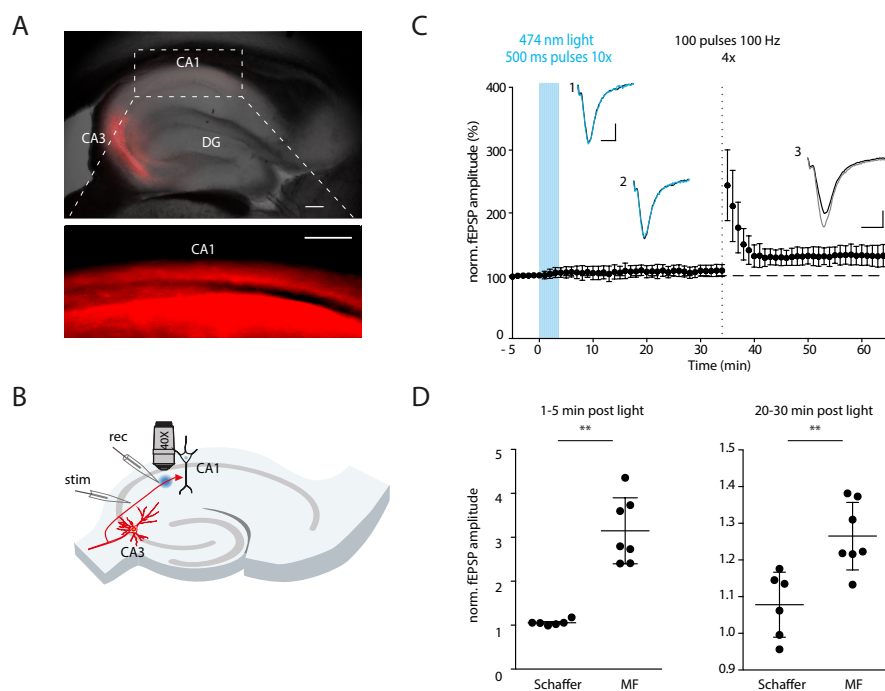


Figure 8. Lack of synaptoPAC effect in Schaffer collateral-CA1 synapses. (A) Overlay of DIC and fluorescent image showing synaptoPAC expression in area CA3 and in Schaffer collaterals (inset). Scale bars: 200 μm . (B) Scheme of the experimental setup for recordings at Schaffer collateral-CA1 synapses, with optical stimulation in *str. radiatum* close to the recording electrode. (C) Time course of Schaffer collateral-fEPSP amplitudes and relative example traces (1) 5 min ($104 \pm 6\%$ of baseline), and (2) 20-30 min ($107 \pm 8\%$) before (black) and after (blue) synaptoPAC activation. After tetanic stimulation (grey) the synapses showed post-tetanic potentiation of $192 \pm 42\%$ and long-term potentiation (3) ($132 \pm 15\%$; $n = 6$ slices, 3 mice). Scale bars: 100 μV , 10 ms. (D) Comparison of the synaptoPAC effect on transmission at MF-CA3 and CA3-CA1 synapses (1-5 min: $p = 0.0006$; 20-30 min: $p = 0.02$, both Mann Whitney test). Data points shown are binned to 1 min. Figure modified from Oldani et al., 2020.

After light stimulation, LTP was induced by tetanic electrical stimulation (4 trains of 100 electrical stimuli at 100 Hz), which increased fEPSP amplitudes, demonstrating the general ability of the synapses to undergo synaptic potentiation. The increase in fEPSP amplitude after photostimulation was statistically higher in MF-CA3 synapses compared to CA3-CA1 synapses, both within 5 min and at 20 to 30 min post light (Fig. 8D). This result indicates that the effect of synaptoPAC is specific to synapses that express a cAMP-dependent type of LTP.

5.5 Optical and pharmacological induction in comparison

Finally, we thought that a direct comparison would be useful to investigate whether synaptoPAC is at least as effective as the classical pharmacological induction of presynaptic LTP by forskolin (FSK). In cultured granule cells, we found that application of FSK (50 μM) at granule cells autapses did not further enhance transmission after synaptoPAC-mediated potentiation (Fig. 9A; EPSC increase: *light*: 1.22 ± 0.22 ; *FSK*: 1.24 ± 0.26 ; $n = 10$, $N = 4$). Conversely, light stimulation did not further potentiate release in granule cells already exposed to FSK (Fig. 9B; EPSCs increase: *FSK*: 1.40 ± 0.48 nA; *light*: 1.44 ± 0.48 ; $n = 12$; $N = 3$). The mutual occlusion of the effects in these experiments indicates that both manipulations saturate the signalling cascade downstream of cAMP.

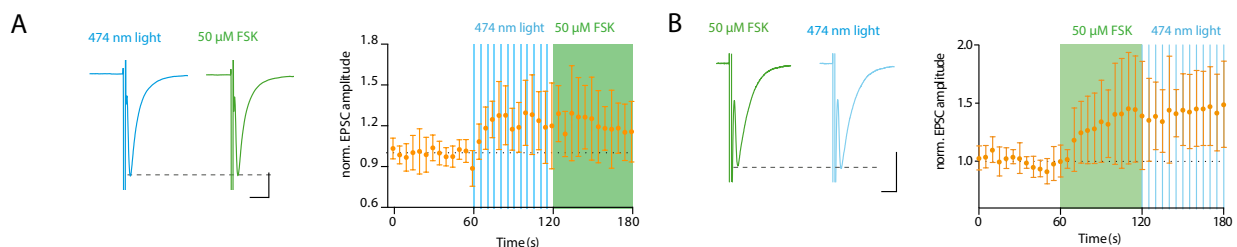


Figure 9. SynaptoPAC and forskolin are equally effective in enhancing synaptic transmission. (A) Potentiation of EPSCs by activation of synaptoPAC (blue) is not further enhanced by subsequent application of 50 μM forskolin (green) in cultured granule cells. Scale bar: 10 ms, 1 nA. (B) Photostimulation did not further increase transmitter release in synaptoPAC-expressing granule cells already treated with forskolin. Scale bar: 10 ms, 0.5 nA. Figure modified from Oldani et al., 2020.

6. Discussion and outlook

In this study we successfully established our newly developed optogenetic tool synaptoPAC as a blue light-sensitive tool for the induction of presynaptic plasticity. We showed that the activation of synaptoPAC is able to potentiate synaptic transmission both in autaptic cultures of hippocampal granule cells and in acute brain slices at MF-CA3 synapses. Since the mechanisms underlying presynaptic potentiation and the role of presynaptic plasticity in behaviour are not yet completely elucidated, we believe that synaptoPAC will greatly facilitate further investigations in this field (Monday et al. 2017). SynaptoPAC is well suited for addressing these questions for several reasons: first, it is a small protein that can be easily expressed both *in vitro* and *in vivo* via lentivirus or AAV. Second, its high sensitivity to blue light allows activation by a wide range of light intensities and by different light protocols (Fig. 6). SynaptoPAC can be activated with short light pulses (25 ms) and with low light intensity ($0.17 \text{ mW}\cdot\text{s}\cdot\text{mm}^{-2}$), suggesting that the tool is well suited for *in vivo* experiments. Finally, we demonstrated that local illumination of axonal terminals expressing synaptoPAC is sufficient to elicit the desired effect (Fig. 6). Since cAMP is an important second messenger, experimental variation of its concentration may exert unintended effects on intracellular signalling cascades, cellular metabolism, and gene expression. The potential to elicit presynaptic potentiation by local illumination of the terminals, together with the presynaptic enrichment of the tool (Fig. 3), is expected to limit adverse cAMP effects by synaptoPAC. From our experience, it is important to minimise exposure of synaptoPAC to background light $<500 \text{ nm}$, because of the BLUF domain's sensitivity to blue light. We therefore recommend to perform experiments under continuous safelight illumination.

In our study we observed that photoinduction of presynaptic potentiation is cell-type specific. In cultured neurons, the increase in EPSC amplitudes upon light stimulation was observed only in granule cells but not in other cell-types (Fig. 5B). Along this line, when synaptoPAC was expressed in acute slices we could induce LTP at MF-CA3 synapses, but not at CA3-CA1 synapses (Fig. 6 and 8). These results are in accordance with a cAMP-mediated induction of presynaptic LTP at specific synapse-types (Zalutsky et Nicoll, 1990, Weisskopf et al., 1994). Previous studies have shown that synapses that display presynaptic plasticity express high levels of adenylyl cyclases, specifically subtype 1 and 8, which seems to be required for long term potentiation (Villacres et al. 1998; Wang et al. 2003). Our data suggest that the intraterminal

increase of cAMP alone is sufficient to induce LTP at MF-CA3 synapses, but not in other synapses such as Schaffer collaterals. This is probably due to the lack of a specific molecular downstream target for cAMP/PKA in the release machinery, or to morphological differences that render these synapses unable to undergo structural changes that are necessary for presynaptic LTP. This characteristic of synaptoPAC can be exploited in dissecting neuronal circuits and, more specifically, to gain more knowledge on which other synapses in the brain need cAMP/PKA signalling for presynaptic LTP induction. It has been indeed shown that the same type of presynaptic neurons projecting onto different postsynaptic cell-types can have different requirements for LTP induction. One example of this phenomenon is the rat cerebellar parallel fibres from granule cells that express presynaptic, cAMP/PKA dependent LTP for projections onto Purkinje cells and molecular layer interneurons (Salin et al., 1996; Bender et al., 2006), but not for projections onto stellate cells (Rancillac and Crépel, 2004). Due to the excellent spatial resolution and the specifically presynaptic expression, synaptoPAC can be used to investigate other synapses in the brain that share a similar mechanism, without side effects at the postsynaptic neurons, which are a caveat of forskolin application.

Moreover the combined use of synaptoPAC with ultrastructural imaging such as flash-and-freeze EM (Imig et al., 2020) can also be exploited to determinate molecular mechanisms underlying the role of cAMP/PKA pathway in structural plasticity. Interestingly, cAMP/PKA was demonstrated to act as regulator of the synaptic vesicle release mode (Vaden et al., 2019), and to promote dense core vesicle release of neuropeptides (Steuer Costa et al., 2017), indicating that cAMP modulates release in various ways.

One limitation of the *in vitro* brain slice experiments presented in this study (Fig. 6, 7 and 8) is that synaptoPAC is most likely not systematically expressed in all fibres in the target area. Therefore, we cannot ensure that all synapses that were electrically stimulated were potentiated after optical stimulation. One way to resolve this issue is to combine, in the same cell, the expression of synaptoPAC and an excitatory opsin. Because of absorption spectra overlap, the channelrhodopsin of choice should be a red-shifted one, such as Chrimson, ReaChR, or variants of these, which allow excitation with light of a wavelength longer than 500 nm (Klapoetke et al., 2014; Lin et al., 2013) and do not interfere with the activation of the BLUF domain of synaptoPAC.

In hippocampal slices, synaptoPAC-mediated potentiation of MF transmission showed a strong initial potentiation, very similar to the post-tetanic potentiation (PTP) previously described in MF-CA3 synapses (Griffith, 1990), that decays over decades of minutes (Fig. 6D and E). Recent studies have started to investigate the physiological significance of PTP as a potential candidate that underlies short-term memory. Specifically, it has been shown that unitary MF-EPSPs fail to initiate spikes in CA3 neurons while during PTP, single MF-EPSPs reliably trigger postsynaptic action potentials (Vyleta et al., 2016), suggesting that PTP can function as a computational switch from a sub-detonation to a full detonation mode for hippocampal MF synapses. More recently, *in vivo* experiments suggested PTP as a phenomenon that occurs naturally during physiological granule cells activity (Vandael et al., 2020). How this altered synaptic computation affects encoding, storage and recall of associative memories is currently unknown (Rebola et al., 2017). We believe that synaptoPAC is the perfect tool for further investigations in this field of research that currently is receiving broad interest. Finally, growing evidence suggests that presynaptic plasticity can be altered in brain diseases such as schizophrenia, autism, addictions and neurodegenerative disorders. Unfortunately, animal models used to study these diseases (for e.g. the 22q11 mouse model for schizophrenia, FMR1 for autism, α -synuclein for Parkinson diseases, etc.), are not sufficient to clarify whether impaired presynaptic plasticity is a cause or a consequence of the diseases (for review, see Monday et al., 2018). We believe that the use of animal models combined with synaptoPAC, which allows for the rescue of a presynaptic phenotype with precise spatiotemporal resolution, could be extremely helpful in unravelling some of the outstanding questions of presynaptic plasticity under pathophysiological conditions.

7. References

- Abbott, L. F., & Regehr, W. G. (2004). Synaptic computation. *Nature*, 431(7010), 796–803.
- Alder, J., Kanki, H., Valtorta, F., Greengard, P., & Poo, M. M. (1995). Overexpression of synaptophysin enhances neurotransmitter secretion at *Xenopus* neuromuscular synapses. *The Journal of neuroscience*, 15(1 Pt 2), 511–519.
- Bernal Sierra, Y. A., Rost, B. R., Pofahl, M., Fernandes, A. M., Kopton, R. A., Moser, S., Holtkamp, D., Masala, N., Beed, P., Tukker, J. J., Oldani, S., Bönigk, W., Kohl, P., Baier, H., Schneider-Warme, F., Hegemann, P., Beck, H., Seifert, R., & Schmitz, D. (2018). Potassium channel-based optogenetic silencing. *Nature communications*, 9(1), 4611.
- Bender, V. A., Pugh, J. R., & Jahr, C. E. (2009). Presynaptically expressed long-term potentiation increases multivesicular release at parallel fiber synapses. *The Journal of neuroscience*, 29(35), 10974–10978.
- Bliss, T. V., & Lomo, T. (1973). Long-lasting potentiation of synaptic transmission in the dentate area of the anaesthetized rabbit following stimulation of the perforant path. *The Journal of physiology*, 232(2), 331–356.
- Brams, M., Kusch, J., Spurny, R., Benndorf, K., & Ulens, C. (2014). Family of prokaryote cyclic nucleotide-modulated ion channels. *Proceedings of the National Academy of Sciences of the United States of America*, 111(21), 7855–7860.
- Castillo P. E. (2012). Presynaptic LTP and LTD of excitatory and inhibitory synapses. *Cold Spring Harbor perspectives in biology*, 4(2), a005728.
- Castro-Alamancos, M. A., & Calcagnotto, M. E. (1999). Presynaptic long-term potentiation in corticothalamic synapses. *The Journal of neuroscience*, 19(20), 9090–9097.
- Chen, H. X., Jiang, M., Akakin, D., & Roper, S. N. (2009). Long-term potentiation of excitatory synapses on neocortical somatostatin-expressing interneurons. *Journal of neurophysiology*, 102(6), 3251–3259.
- De Armentia, M., & Sah, P. (2007). Bidirectional synaptic plasticity at nociceptive afferents in the rat central amygdala. *The Journal of physiology*, 581(Pt 3), 961–970.
- Griffith W. H. (1990). Voltage-clamp analysis of posttetanic potentiation of the mossy fiber to CA3 synapse in hippocampus. *Journal of neurophysiology*, 63(3), 491–501.
- Harris, E. W., & Cotman, C. W. (1986). Long-term potentiation of guinea pig mossy fiber responses is not blocked by N-methyl d-aspartate antagonists. *Neuroscience Letters*, 70(1), 132–137.
- Huang, Y. Y., Kandel, E. R., Varshavsky, L., Brandon, E. P., Qi, M., Idzerda, R. L., McKnight, G. S., & Bourtschouladze, R. (1995). A genetic test of the effects of mutations in PKA on mossy fiber LTP and its relation to spatial and contextual learning. *Cell*, 83(7), 1211–1222.
- Imig, C., López-Murcia, F. J., Maus, L., García-Plaza, I. H., Mortensen, L. S., Schwark, M., Schwarze, V., Angibaud, J., Nägerl, U. V., Taschenberger, H., Brose, N., & Cooper, B. H. (2020). Ultrastructural Imaging of Activity-Dependent Synaptic Membrane-Trafficking Events in Cultured Brain Slices. *Neuron*, 108(5), 843–860.e8.
- Iseki, M., Matsunaga, S., Murakami, A., Ohno, K., Shiga, K., Yoshida, K., Sugai, M., Takahashi, T., Hori, T., & Watanabe, M. (2002). A blue-light-activated adenylyl cyclase mediates photoavoidance in *Euglena gracilis*. *Nature*, 415(6875), 1047–1051.
- Kamiya, H., Shinozaki, H., & Yamamoto, C. (1996). Activation of metabotropic glutamate receptor type 2/3 suppresses transmission at rat hippocampal mossy fibre synapses. *The Journal of physiology*, 493 (Pt 2)(Pt 2), 447–455.
- Kees, A. L., Marneffe, C., & Mulle, C. (2020). Lighting up pre-synaptic potentiation: An Editorial for "SynaptoPAC, an optogenetic tool for induction of presynaptic plasticity" on <https://doi.org/10.1111/jnc.15210>. *Journal of neurochemistry*, 10.1111/jnc.15236.
- Klapoetke, N. C., Murata, Y., Kim, S. S., Pulver, S. R., Birdsey-Benson, A., Cho, Y. K., Morimoto, T. K., Chuong, A. S., Carpenter, E. J., Tian, Z., Wang, J., Xie, Y., Yan, Z., Zhang, Y., Chow, B. Y., Surek, B., Melkonian, M., Jayaraman, V., Constantine-Paton, M., Wong, G. K., Boyden, E. S. (2014). Independent optical excitation of distinct neural populations. *Nature methods*, 11(3), 338–346.
- Korte, M., & Schmitz, D. (2016). Cellular and System Biology of Memory: Timing, Molecules, and Beyond. *Physiological reviews*, 96(2), 647–693.

- Lin, J. Y., Knutsen, P. M., Muller, A., Kleinfeld, D., & Tsien, R. Y. (2013). ReaChR: a red-shifted variant of channelrhodopsin enables deep transcranial optogenetic excitation. *Nature neuroscience*, *16*(10), 1499–1508.
- Liu, X., Ramirez, S., Pang, P. T., Puryear, C. B., Govindarajan, A., Deisseroth, K., & Tonegawa, S. (2012). Optogenetic stimulation of a hippocampal engram activates fear memory recall. *Nature*, *484*, 381–385.
- Martin, S. J., Grimwood, P. D., & Morris, R. G. (2000). Synaptic plasticity and memory: an evaluation of the hypothesis. *Annual review of neuroscience*, *23*, 649–711.
- Monday, H. R., & Castillo, P. E. (2017). Closing the gap: long-term presynaptic plasticity in brain function and disease. *Current opinion in neurobiology*, *45*, 106–112.
- Monday, H. R., Younts, T. J., & Castillo, P. E. (2018). Long-Term Plasticity of Neurotransmitter Release: Emerging Mechanisms and Contributions to Brain Function and Disease. *Annual review of neuroscience*, *41*, 299–322.
- Nabavi, S., Fox, R., Proulx, C. D., Lin, J. Y., Tsien, R. Y., & Malinow, R. (2014). Engineering a memory with LTD and LTP. *Nature*, *511*(7509), 348–352.
- Nicoll, R. A., & Schmitz, D. (2005). Synaptic plasticity at hippocampal mossy fibre synapses. *Nature reviews. Neuroscience*, *6*(11), 863–876.
- Oldani, S., Moreno-Velasquez, L., Faiss, L., Stumpf, A., Rosenmund, C., Schmitz, D., & Rost, B. R. (2020). SynaptoPAC, an optogenetic tool for induction of presynaptic plasticity. *Journal of neurochemistry*, *10.1111/jnc.15210*.
- Rancillac, A., & Crépel, F. (2004). Synapses between parallel fibres and stellate cells express long-term changes in synaptic efficacy in rat cerebellum. *The Journal of physiology*, *554*(Pt 3), 707–720.
- Ramirez, S., Liu, X., Lin, P. A., Suh, J., Pignatelli, M., Redondo, R. L., Ryan, T. J., & Tonegawa, S. (2013). Creating a false memory in the hippocampus. *Science*, *341*(6144), 387–391.
- Rebola, N., Carta, M., & Mulle, C. (2017). Operation and plasticity of hippocampal CA3 circuits: implications for memory encoding. *Nature reviews. Neuroscience*, *18*(4), 208–220.
- Rost B. R., Breustedt J, Schoenherr A, Grosse G, Ahnert-Hilger G, Schmitz D. (2010). Autaptic cultures of single hippocampal granule cells of mice and rats. *European Journal of Neuroscience*, *32*, 939–947.
- Rost, B. R., Schneider, F., Grauel, M. K., Wozny, C., Bentz, C., Blessing, A., Rosenmund, T., Jentsch, T. J., Schmitz, D., Hegemann, P., & Rosenmund, C. (2015). Optogenetic acidification of synaptic vesicles and lysosomes. *Nature neuroscience*, *18*(12), 1845–1852.
- Salin, P. A., Malenka, R. C., & Nicoll, R. A. (1996). Cyclic AMP mediates a presynaptic form of LTP at cerebellar parallel fiber synapses. *Neuron*, *16*(4), 797–803.
- Shcherbo, D., Murphy, C. S., Ermakova, G. V., Solovieva, E. A., Chepurnykh, T. V., Shcheglov, A. S., Verkhusha, V. V., Pletnev, V. Z., Hazelwood, K. L., Roche, P. M., Lukyanov, S., Zaraisky, A. G., Davidson, M. W., & Chudakov, D. M. (2009). Far-red fluorescent tags for protein imaging in living tissues. *The Biochemical journal*, *418*(3), 567–574.
- Schindelin, J., Arganda-Carreras, I., Frise, E., Kaynig, V., Longair, M., Pietzsch, T., Preibisch, S., Rueden, C., Saalfeld, S., Schmid, B., Tinevez, J. Y., White, D. J., Hartenstein, V., Eliceiri, K., Tomancak, P., & Cardona, A. (2012). Fiji: an open-source platform for biological-image analysis. *Nature methods*, *9*(7), 676–682.
- Staubli, U., Larson, J., & Lynch, G. (1990). Mossy fiber potentiation and long-term potentiation involve different expression mechanisms. *Synapse*, *5*(4), 333–335.
- Steuer Costa, W., Yu, S. C., Liewald, J. F., & Gottschalk, A. (2017). Fast cAMP Modulation of Neurotransmission via Neuropeptide Signals and Vesicle Loading. *Current biology : CB*, *27*(4), 495–507.
- Stierl, M., Stumpf, P., Udvari, D., Gueta, R., Hagedorn, R., Losi, A., Gärtner, W., Petereit, L., Efetova, M., Schwarzel, M., Oertner, T. G., Nagel, G., & Hegemann, P. (2011). Light modulation of cellular cAMP by a small bacterial photoactivated adenylyl cyclase, bPAC, of the soil bacterium *Beggiatoa*. *The Journal of biological chemistry*, *286*(2), 1181–1188.
- Vaden, J. H., Banumurthy, G., Gusarevich, E. S., Overstreet-Wadiche, L., & Wadiche, J. I. (2019). The readily-releasable pool dynamically regulates multivesicular release. *eLife*, *8*, e47434.
- Vandael, D., Borges-Merjane, C., Zhang, X. and Jonas, P. (2020). Short-Term Plasticity at Hippocampal Mossy Fiber Synapses Is Induced by Natural Activity Patterns and Associated with Vesicle Pool Engram Formation. *Neuron*, *107*, 509-521 e507.

- Villacres, E. C., Wong, S. T., Chavkin, C., & Storm, D. R. (1998). Type I adenylyl cyclase mutant mice have impaired mossy fiber long-term potentiation. *The Journal of neuroscience*, 18(9), 3186–3194.
- Vyleta, N. P., Borges-Merjane, C., & Jonas, P. (2016). Plasticity-dependent, full detonation at hippocampal mossy fiber-CA3 pyramidal neuron synapses. *eLife*, 5, e17977.
- Wang, H., Pineda, V. V., Chan, G. C., Wong, S. T., Muglia, L. J., & Storm, D. R. (2003). Type 8 adenylyl cyclase is targeted to excitatory synapses and required for mossy fiber long-term potentiation. *The Journal of neuroscience*, 23(30), 9710–9718.
- Weisskopf, M. G., Castillo, P. E., Zalutsky, R. A. and Nicoll, R. A. (1994). Mediation of hippocampal mossy fiber long-term potentiation by cyclic AMP. *Science*, 265, 1878-1882.
- Wozny, C., Maier, N., Fidzinski, P., Breustedt, J., Behr, J. and Schmitz, D. (2008). Differential cAMP signaling at hippocampal output synapses. *The Journal of neuroscience*, 28, 14358-14362.
- Zalutsky, R. A. and Nicoll, R. A. (1990). Comparison of two forms of long-term potentiation in single hippocampal neurons. *Science*, 248, 1619-1624.

8. Affidavit

“I, Silvia Oldani, by personally signing this document in lieu of an oath, hereby affirm that I prepared the submitted dissertation on the topic optical induction of presynaptic plasticity using synaptoPAC/Optische Induktion präsynaptischer Plastizität mittels synaptoPAC, independently and without the support of third parties, and that I used no other sources and aids than those stated.

All parts which are based on the publications or presentations of other authors, either in letter or in spirit, are specified as such in accordance with the citing guidelines. The sections on methodology (in particular regarding practical work, laboratory regulations, statistical processing) and results (in particular regarding figures, charts and tables) are exclusively my responsibility.

Furthermore, I declare that I have correctly marked all of the data, the analyses, and the conclusions generated from data obtained in collaboration with other persons, and that I have correctly marked my own contribution and the contributions of other persons (cf. declaration of contribution). I have correctly marked all texts or parts of texts that were generated in collaboration with other persons.

My contributions to any publications to this dissertation correspond to those stated in the below joint declaration made together with the supervisor. All publications created within the scope of the dissertation comply with the guidelines of the ICMJE (International Committee of Medical Journal Editors; www.icmje.org) on authorship. In addition, I declare that I shall comply with the regulations of Charité – Universitätsmedizin Berlin on ensuring good scientific practice.

I declare that I have not yet submitted this dissertation in identical or similar form to another Faculty.

The significance of this statutory declaration and the consequences of a false statutory declaration under criminal law (Sections 156, 161 of the German Criminal Code) are known to me.”

Date

Signature

9. Detailed Declaration of Contribution

Silvia Oldani contributed the following to the below listed publication:

Publication: Oldani, S., Moreno-Velasquez, L., Faiss, L., Stumpf, A., Rosenmund, C., Schmitz, D., & Rost, B. R. (2020). SynptoPAC, an optogenetic tool for induction of presynaptic plasticity. *Journal of neurochemistry*, 10.1111/jnc.15210.

Contribution in detail:

Planning of the experiments

Conception of the project: Benjamin Rost and Dietmar Schmitz

Design of the tool: Benjamin Rost

Planning of the electrophysiology experiments: Silvia Oldani, Benjamin Rost and Dietmar Schmitz.

Execution of experiments

Molecular biology: Anke Schönherr, Katja Pötschke and Bettina Brokowski

Preparation of ND7/23 cells: Benjamin Rost

Preparation of cultured granule cells: Silvia Oldani, Anke Schönherr and Katja Czielesky

Whole-cell recordings from ND7/23 cells: Benjamin Rost (Fig. 1)

Whole-cell recordings from cultured neurons: Silvia Oldani (Fig. 2, Suppl Fig. 3), Benjamin Rost (Suppl Fig. 1, Suppl Fig. 2), Lukas Faiss (Suppl Fig. 1, Suppl Fig. 2)

In vivo viral injections: Silvia Oldani (Fig. 3, Fig. 4, Suppl Fig. 4) with support of Katja Czielesky

Preparation of mouse hippocampal slices: Silvia Oldani (Fig. 3, Fig. 4, Suppl Fig. 4, Suppl Fig. 5)

Field potential recordings of Mossy fibres: Silvia Oldani (Fig. 3, Fig. 4, Suppl Fig. 4, Suppl Fig. 5), Moreno-Velasquez L (Fig. 3, Suppl Fig. 4, Suppl Fig. 5) Stumpf A (Suppl Fig. 5)

Field potential recordings of Schaffer collaterals: Silvia Oldani (Fig. 3)

Immunostainings: Silvia Oldani (Fig. 1)

Confocal imaging: Silvia Oldani, Lukas Faiss (Fig. 1)

Data Analysis

Data obtained from ND7/23 cell recordings: Benjamin Rost (Fig. 1)

Analysis of data from neuronal culture recordings: Silvia Oldani (Fig. 2, Suppl Fig. 3) Benjamin Rost (Suppl Fig. 1, Suppl Fig. 2).

Analysis of recordings in brain slices: Silvia Oldani (Fig. 3, Fig. 4, Suppl Fig. 4, Suppl Fig. 5)

Analysis of synaptic enrichment: Lukas Faiss (Fig. 1).

Data visualisation

Silvia Oldani and Benjamin Rost.

Writing and editing of the manuscript

Benjamin Rost and Silvia Oldani together with Dietmar Schmitz with inputs from all the authors.

Signature, date and stamp of the doctoral supervisor

Signature of the doctoral candidate

10. ISI Web of Knowledge Journal Citation Report

Journal Data Filtered By: **Selected JCR Year: 2018** Selected Editions: SCIE,SSCI
 Selected Categories: **"BIOCHEMISTRY and MOLECULAR BIOLOGY"** Selected
 Category Scheme: WoS
Gesamtanzahl: 298 Journale

Rank	Full Journal Title	Total Cites	Journal Impact Factor	Eigenfactor Score
1	CELL	242,829	36.216	0.571850
2	NATURE MEDICINE	79,243	30.641	0.162840
3	Annual Review of Biochemistry	20,344	26.922	0.025450
4	TRENDS IN BIOCHEMICAL SCIENCES	17,448	16.889	0.031380
5	MOLECULAR BIOLOGY AND EVOLUTION	46,915	14.797	0.092200
6	MOLECULAR CELL	62,812	14.548	0.170680
7	PROGRESS IN LIPID RESEARCH	5,839	12.540	0.007160
8	Nature Chemical Biology	21,428	12.154	0.061180
9	NATURE STRUCTURAL & MOLECULAR BIOLOGY	27,166	12.109	0.069440
10	TRENDS IN MICROBIOLOGY	12,514	11.974	0.020700
11	MOLECULAR PSYCHIATRY	20,353	11.973	0.049290
12	NATURAL PRODUCT REPORTS	11,039	11.876	0.014870
13	EMBO JOURNAL	65,212	11.227	0.067930
14	NUCLEIC ACIDS RESEARCH	181,592	11.147	0.402620
15	TRENDS IN MOLECULAR MEDICINE	9,946	11.028	0.018900
16	Molecular Plant	9,274	10.812	0.027150
17	Molecular Cancer	11,626	10.679	0.021350
18	GENOME RESEARCH	39,240	9.944	0.079580
19	Molecular Systems Biology	8,936	9.800	0.019680
20	CURRENT BIOLOGY	60,772	9.193	0.135820
21	Cell Systems	2,275	8.640	0.016280








Rank	Full Journal Title	Total Cites	Journal Impact Factor	Eigenfactor Score
22	PLANT CELL	52,034	8.631	0.057800
23	CURRENT OPINION IN CHEMICAL BIOLOGY	10,499	8.544	0.018990
24	PLOS BIOLOGY	29,974	8.386	0.057950
25	EMBO REPORTS	13,786	8.383	0.029850
26	MOLECULAR ASPECTS OF MEDICINE	5,568	8.313	0.009020
27	CELL DEATH AND DIFFERENTIATION	19,729	8.086	0.030290
28	Redox Biology	7,192	7.793	0.019620
29	CURRENT OPINION IN STRUCTURAL BIOLOGY	11,066	7.052	0.024160
30	Molecular Ecology Resources	10,473	7.049	0.019000
31	CELLULAR AND MOLECULAR LIFE SCIENCES	24,422	7.014	0.038970
32	MATRIX BIOLOGY	5,699	6.986	0.009540
33	BIOCHIMICA ET BIOPHYSICA ACTA-REVIEWS ON CANCER	5,226	6.887	0.008260
34	Cell Chemical Biology	2,022	6.762	0.009380
35	ONCOGENE	63,249	6.634	0.074600
36	Science Signaling	11,403	6.481	0.033700
37	Reviews of Physiology Biochemistry and Pharmacology	738	6.214	0.000540
38	CRITICAL REVIEWS IN BIOCHEMISTRY AND MOLECULAR BIOLOGY	3,489	6.069	0.006540
39	Signal Transduction and Targeted Therapy	371	5.873	0.000990
40	MOLECULAR ECOLOGY	39,464	5.855	0.060180
41	ANTIOXIDANTS & REDOX SIGNALING	20,275	5.828	0.029700
42	BIOMACROMOLECULES	37,954	5.667	0.037180
43	FREE RADICAL BIOLOGY AND MEDICINE	40,820	5.657	0.040300

Rank	Full Journal Title	Total Cites	Journal Impact Factor	Eigenfactor Score
44	RNA Biology	5,855	5.477	0.018620
45	CYTOKINE & GROWTH FACTOR REVIEWS	5,688	5.458	0.007680
46	FASEB JOURNAL	41,854	5.391	0.047670
47	JOURNAL OF MOLECULAR BIOLOGY	57,921	5.067	0.042100
48	AMYLOID-JOURNAL OF PROTEIN FOLDING DISORDERS	1,335	4.919	0.003270
49	JOURNAL OF NEUROCHEMISTRY	35,902	4.870	0.026140
50	Essays in Biochemistry	1,674	4.845	0.003010
51	CURRENT OPINION IN LIPIDOLOGY	4,140	4.844	0.006320
52	INTERNATIONAL JOURNAL OF BIOLOGICAL MACROMOLECULES	31,707	4.784	0.040180
53	EXPERIMENTAL AND MOLECULAR MEDICINE	4,046	4.743	0.007380
53	JOURNAL OF LIPID RESEARCH	23,523	4.743	0.025090
55	BIOCHIMICA ET BIOPHYSICA ACTA-MOLECULAR CELL RESEARCH	16,440	4.739	0.030020
55	FEBS Journal	18,035	4.739	0.033180
57	Computational and Structural Biotechnology Journal	1,363	4.720	0.004810
58	Biomolecules	2,274	4.694	0.008300
59	Journal of Genetics and Genomics	2,005	4.650	0.004740
60	Biochimica et Biophysica Acta-Gene Regulatory Mechanisms	7,096	4.599	0.015580
61	STRUCTURE	14,722	4.576	0.031710
62	HUMAN MOLECULAR GENETICS	39,859	4.544	0.069190
63	Antioxidants	882	4.520	0.001690
64	JOURNAL OF NUTRITIONAL BIOCHEMISTRY	10,544	4.490	0.012700

11. Publication

Oldani, S., Moreno-Velasquez, L., Faiss, L., Stumpf, A., Rosenmund, C., Schmitz, D., & Rost, B. R. (2020). SynaptoPAC, an optogenetic tool for induction of presynaptic plasticity. *Journal of neurochemistry*, 10.1111/jnc.15210.

SynaptoPAC, an optogenetic tool for induction of presynaptic plasticity

Silvia Oldani^{1,2}  | Laura Moreno-Velasquez²  | Lukas Faiss^{1,2}  | Alexander Stumpf²  |
Christian Rosenmund²  | Dietmar Schmitz^{1,2,3,4,5}  | Benjamin R. Rost¹ 

¹German Center for Neurodegenerative Diseases (DZNE), Berlin, Germany

²Charité – Universitätsmedizin Berlin, corporate member of Freie Universität Berlin and Humboldt-Universität zu Berlin, and Berlin Institute of Health, NeuroCure Cluster of Excellence, Berlin, Germany

³Max-Delbrück-Centrum (MDC) for Molecular Medicine in the Helmholtz Association, Berlin, Germany

⁴Bernstein Center for Computational Neuroscience, Berlin, Germany

⁵Einstein Center for Neurosciences Berlin, Berlin, Germany

Correspondence

Dietmar Schmitz and Benjamin R. Rost, German Center for Neurodegenerative Diseases (DZNE), 10117 Berlin, Germany. Email: dietmar.schmitz@charite.de (or) benjamin.rost@dzne.de

Funding information

Deutsche Forschungsgemeinschaft, Grant/Award Number: 390688087, SPP 1926, SPP 1665, SFB 1315 and SFB 958

Read the Editorial Highlight for this article on: <https://doi.org/10.1111/jnc.15236>

Abstract

Optogenetic manipulations have transformed neuroscience in recent years. While sophisticated tools now exist for controlling the firing patterns of neurons, it remains challenging to optogenetically define the plasticity state of individual synapses. A variety of synapses in the mammalian brain express presynaptic long-term potentiation (LTP) upon elevation of presynaptic cyclic adenosine monophosphate (cAMP), but the molecular expression mechanisms as well as the impact of presynaptic LTP on network activity and behavior are not fully understood. In order to establish optogenetic control of presynaptic cAMP levels and thereby presynaptic potentiation, we developed synaptoPAC, a presynaptically targeted version of the photoactivated adenylyl cyclase bPAC. In cultures of hippocampal granule cells of Wistar rats, activation of synaptoPAC with blue light increased action potential-evoked transmission, an effect not seen in hippocampal cultures of non-granule cells. In acute brain slices of C57BL/6N mice, synaptoPAC activation immediately triggered a strong presynaptic potentiation at mossy fiber synapses in CA3, but not at Schaffer collateral synapses in CA1. Following light-triggered potentiation, mossy fiber transmission decreased within 20 min, but remained enhanced still after 30 min. The optogenetic potentiation altered the short-term plasticity dynamics of release, reminiscent of presynaptic LTP. Our work establishes synaptoPAC as an optogenetic tool that enables acute light-controlled potentiation of transmitter release at specific synapses in the brain, facilitating studies of the role of presynaptic potentiation in network function and animal behavior in an unprecedented manner.

KEYWORDS

dentate gyrus, hippocampus, long-term potentiation, optogenetics, presynaptic plasticity

Abbreviations: ACSF, artificial cerebrospinal fluid; bPAC, *Beggiatoa* photoactivated adenylyl cyclase; cAMP, cyclic adenosine monophosphate; EPSC, excitatory postsynaptic current; fEPSP, field excitatory postsynaptic potential; mEPSC, miniature excitatory postsynaptic current; MF, mossy fiber; PPR, paired-pulse ratio; Pvr, vesicular release probability; synaptoPAC, synaptic photoactivated adenylyl cyclase.

This is an open access article under the terms of the Creative Commons Attribution-NonCommercial License, which permits use, distribution and reproduction in any medium, provided the original work is properly cited and is not used for commercial purposes.

© 2020 The Authors. Journal of Neurochemistry published by John Wiley & Sons Ltd on behalf of International Society for Neurochemistry

1 | INTRODUCTION

Long-term plasticity of synaptic transmission is considered as the cellular basis of learning and memory (Takeuchi et al., 2014). Specific patterns of activity can lead to strengthening or weakening of synapses on timescales ranging from minutes to days, thereby shaping the functional connectivity of neuronal ensembles. While postsynaptic plasticity involves changes in the number of receptors (Herring & Nicoll, 2016), presynaptic plasticity alters the transmitter release probability or the number of release sites (Monday et al., 2018). At several synapses in the mammalian central nervous system, presynaptic long-term potentiation (LTP) is initiated by an increase in cyclic adenosine monophosphate (cAMP) produced by calcium-stimulated adenylyl cyclases in the presynaptic terminal (Castillo, 2012; Ferguson & Storm, 2004). This process was first described for hippocampal mossy fiber (MF) synapses in CA3 (Huang et al., 1994; Weisskopf et al., 1994; Zalutsky & Nicoll, 1990), and subsequently for several other synapses, for example, the synapses between cerebellar parallel fibers and Purkinje cells (Salin et al., 1996), hippocampal CA1 pyramidal neurons and subiculum burst-firing cells (Wozny et al., 2008), hippocampal mossy cells and granule cells (Hashimoto et al., 2017), cortical afferents to the thalamus and the lateral amygdala (Castro-Alamancos & Calcagnotto, 1999; Fourcaudot et al., 2008; Huang & Kandel, 1998), and the inhibitory synapses between cerebellar stellate cells (Lachamp et al., 2009).

The mechanisms of presynaptic LTP were studied most extensively at MF-CA3 synapses, formed between the axons of dentate gyrus granule cells and the dendrites of CA3 pyramidal cells (Nicoll & Schmitz, 2005). Here, high-frequency electrical stimulation of axons elicits first a strong post-tetanic potentiation of transmitter release, which decays within tens of minutes and is followed by LTP expressed as long-lasting increase of transmission. Alternatively, direct pharmacological activation of adenylyl cyclases by forskolin or application of the cAMP analogue Sp-cAMPS induces a sustained presynaptic potentiation (Huang et al., 1994; Tong et al., 1996; Weisskopf et al., 1994). The increase of presynaptic cAMP activates protein kinase A (PKA) and the guanine nucleotide exchange factor EPAC2 (Fernandes et al., 2015; Weisskopf et al., 1994). Several presynaptic molecules, including RIM1 α , Rab3A, Munc13-1, and synaptotagmin12, have been postulated as downstream targets of cAMP (Castillo et al., 1997, 2002; Kaeser-Woo et al., 2013; Yang &

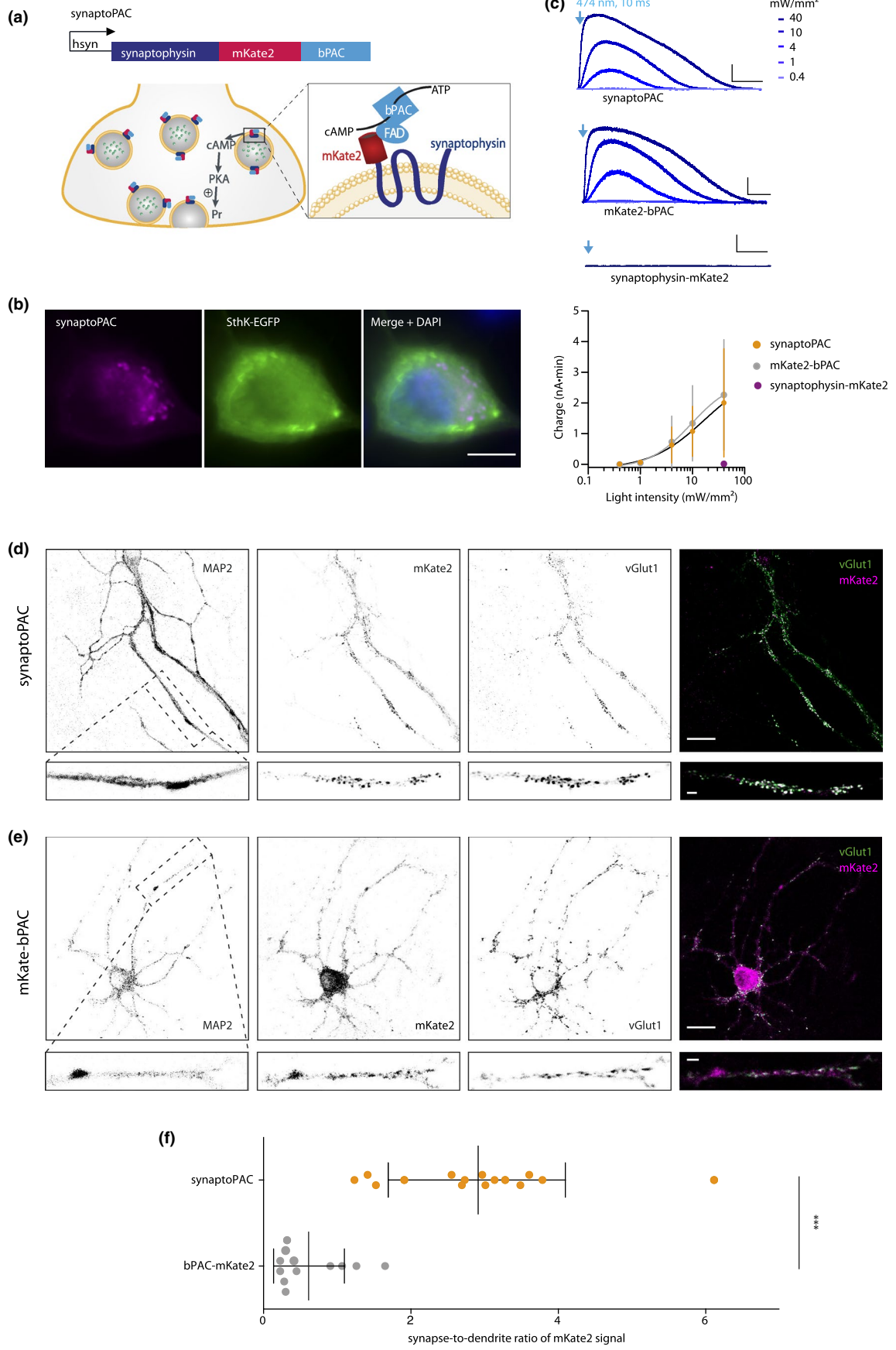
Significance statement

SynaptoPAC is a novel optogenetic tool that allows increasing synaptic transmission by light-controlled induction of presynaptic plasticity.

Calakos, 2011), but despite decades of research, the exact mechanisms of presynaptic long-term potentiation remain elusive.

Both electrical and pharmacological inductions of presynaptic potentiation are not cell-type-specific and difficult to implement in living animals. This lack of minimally invasive and cell-specific tools for controlling presynaptic short- and long-term potentiation is one of the reasons why the computational and behavioral relevance of presynaptic LTP is largely unclear (Monday et al., 2018). To fill this gap, here we establish an optogenetic tool for cell-type-specific manipulation of presynaptic plasticity directly at the axonal terminal. Optogenetic manipulations overcome many of the shortcomings of classical electrical or pharmacological interventions, as they allow cell-type-specific manipulations of biochemical or electrical processes with high spatiotemporal precision, which can be further refined by subcellular targeting strategies (Rost et al., 2017). We reasoned that targeting a photoactivated adenylyl cyclase to the presynaptic terminal would enable light-induced cAMP production in axonal terminals, triggering presynaptic plasticity. The small photoactivated adenylyl cyclase bPAC from *Beggiatoa* has several advantageous features for such an approach, as it is highly sensitive to blue light, shows low dark activity, exhibits a >100 fold increased activity in light, and is well expressed in neurons (Stierl et al., 2011). By fusing bPAC to the synaptic vesicle protein synaptophysin, we created synaptoPAC, a presynaptically targeted version of bPAC (Figure 1a). We demonstrate that light-triggered activation of synaptoPAC elicits presynaptic potentiation, both in autaptic cultures of hippocampal granule cells as well as in field-recordings of hippocampal MFs in acute brain slices. The effect of synaptoPAC activation was vastly different between synapses known for cAMP-dependent modulation of transmission and cAMP-insensitive synaptic terminals, highlighting the specificity of the optogenetic manipulation. Thus, synaptoPAC will likely be of great value for investigations on the mechanisms and functional implications of presynaptic plasticity.

FIGURE 1 Design and validation of synaptoPAC. (a) Illustration of the presynaptic targeting strategy for bPAC, and the optogenetic induction of presynaptic plasticity by synaptoPAC activation. hsyn: human synapsin promoter; FAD: flavin adenine dinucleotide. (b) Fluorescence images of an ND7/23 cell expressing synaptoPAC and SthK-EGFP. Scale bar: 10 μ m. (c) 10 ms flashes of 474 nm light triggered intensity-dependent outward currents in ND7/23 cells co-expressing the cAMP-gated SthK channel together with synaptoPAC ($n = 8$, $N = 2$) or untargeted bPAC ($n = 8$, $N = 2$), but not in cells expressing synaptophysin-mKate2 and SthK. Scale bars: 200 pA, 20 s. (d) Immunofluorescence images of synaptoPAC-expressing cultured neurons stained for the dendritic marker MAP-2, mKate2 indicating synaptoPAC localization, and VGLUT1 as marker for glutamatergic presynaptic terminals. Scale bar: 20 μ m. Close up of a dendrite reveals a signal overlap (white in merge) of mKate2 (magenta) and VGLUT1 (green). MAP2 is not shown in the merge. Scale bar: 2 μ m. (e) Immunofluorescence images of cultured neurons expressing mKate2-bPAC. Scale bars: 20 μ m and 2 μ m for the close up. (f) The average synapse to dendrite ratio of the mKate2 signal was 4.7 times higher for synaptoPAC than for the untargeted mKate2-bPAC (synaptoPAC: 2.9 ± 1.2 , $n = 15$; $N = 3$; mKate2-bPAC: 0.6 ± 0.5 , $n = 12$; $N = 3$; $p < .0001$, Mann-Whitney U test).



2 | MATERIALS AND METHODS

2.1 | Animal experiments

All animal experiments were carried out according to the guidelines stated in Directive 2010/63/EU of the European Parliament on the protection of animals used for scientific purposes and were approved by the local authorities in Berlin (Berlin state government/Landesamt für Gesundheit und Soziales, license number G0092/15, T0100/03 and T0073/04), Germany. Animals were bred in the Charité animal facility and housed in singularly ventilated cages of

4–10 mice on a 12-hr light-dark cycle with access to food and water *ad libitum*.

2.2 | Molecular biology

For initial tests in neuronal cell cultures, we fused the coding sequence of mKate2 and bPAC (from the soil bacterium *Beggiatoa*) to the 3' end of the rat synaptophysin coding sequence by Gibson assembly. The resulting fusion construct (synaptophysin-mKate2-bPAC) was then transferred into a lentiviral expression vector via

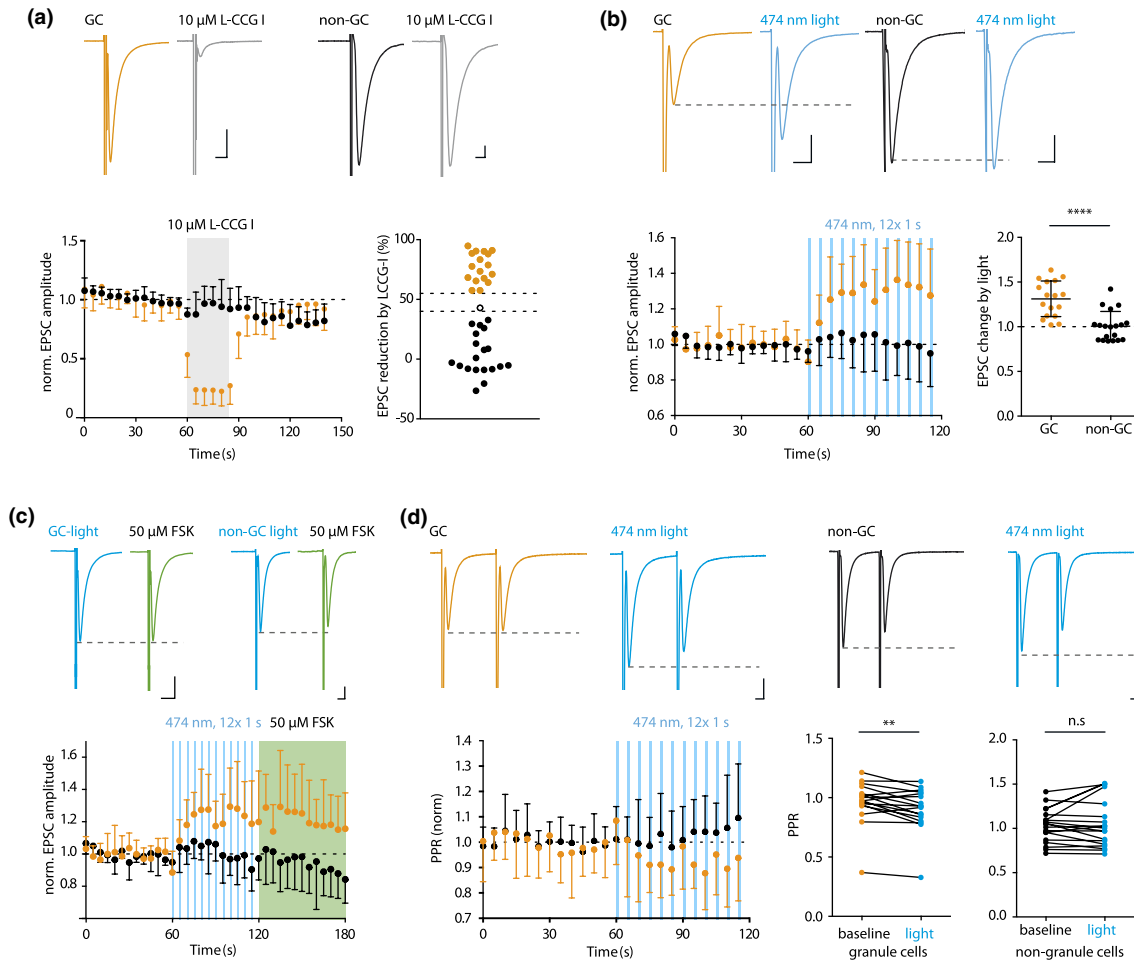


FIGURE 2 SynaptoPAC potentiates evoked synaptic transmission specifically in cultured hippocampal granule cells. (a) Example traces illustrating the effect of the group II metabotropic glutamate receptor agonist L-CCG I (10 μM) on two types of hippocampal excitatory neurons in autaptic cultures. Scale bars, 10 ms, 1 nA. Neurons in which L-CCG I decreased the EPSC amplitude by >55% were classified as granule cells (GCs). Cells with <40% reduction of the EPSC amplitude by L-CCG I were defined as non-granule cells (non-GCs), others (open circle) were not included in further analysis. Time plot shows the reversible L-CCG I effect on EPSC amplitudes recorded from GCs (orange; $n = 17$, $N = 4$) and non-GCs (black; $n = 19$, $N = 5$). (b) EPSCs recorded before and after synaptoPAC activation from a GC and non-GC. Scale bars: 10 ms, 1 nA. Light pulses (474 nm, 70 mW mm⁻², 12 × 1 s at 0.2 Hz) increased EPSC amplitudes in synaptoPAC-expressing GCs by 1.31 ± 0.19 (orange; $n = 17$, $N = 4$), but had no effect in synaptoPAC-expressing non-GCs (black; 1.00 ± 0.16 , $n = 19$, $N = 5$; $p < .0001$; unpaired *t*-test). (c) Potentiation of EPSCs by activation of synaptoPAC (blue) and by subsequent application of 50 μM forskolin (FSK; green). Scale bars: 10 ms, 1 nA. In GCs, FSK increased the EPSC amplitude by 1.21 ± 0.07 (orange; $n = 10$, $N = 4$), not further increasing light induced potentiation. In non-GCs FSK did not increase EPSCs (0.94 ± 0.06 ; black; $n = 9$, $N = 3$). (d) Paired EPSCs evoked at 25 Hz in a GC (orange) and a non-GC (black). Scale bars: 1 nA, 10 ms. Light stimulation significantly decreased the paired-pulse ratio in GCs (baseline: 0.96 ± 0.18 , light: 0.90 ± 0.18 ; $n = 17$, $N = 4$; $p = .005$; Wilcoxon test) but had no effect on the paired-pulse ratio in non-GC (baseline: 1.03 ± 0.18 , light: 1.06 ± 0.27 ; $n = 19$, $N = 5$; $p = .5$, paired *t*-test).

PCR, which allowed expression under control of the neuron-specific human synapsin (hsyn) promoter. This construct was used for the characterization in neuronal cultures (Figures 1 and 2). Since mKate2-fluorescence was very weak and difficult to detect in live-cell imaging, we replaced the fluorophore with mCherry, and transferred the construct into an adeno-associated virus (AAV)-expression vector for more efficient expression of synaptoPAC *in vivo*. In a final step of optimization, we replaced mCherry with mScarlet, since mCherry caused unintended protein aggregations in neurons (data not shown). All viruses (lentivirus and AAV serotype 9) were provided by the Viral Core Facility at the Charité Berlin.

2.3 | Autaptic granule cell culture

Autaptic cultures of dentate gyrus granule cells were prepared as previously described (Rost et al., 2010). In brief, P0-P1 Wistar rats (RRID:RGD_8553003, in total 23 rats) of either sex were decapitated, and brains were removed and transferred into an ice-cooled petri dish. Dentate gyri were dissected by longitudinal separation from the rest of the hippocampus. Cells were isolated by Papain digestion followed by manual trituration, and subsequently plated on islands of glial cells at a density of 1.25×10^4 cells/cm² in 6-well plates in Neurobasal-A (cat. no. 10888022), supplemented with 2% B27 (cat. no. 17504001) and 0.2% penicillin/streptomycin (cat. no. 15140122; all Invitrogen/ Thermo Fisher Scientific, Waltham, MA). Lentiviral particles encoding synaptoPAC were added 1–4 days after plating. Cells were used for electrophysiological recordings after 15–21 days *in vitro*.

2.4 | Cell culture of ND7/23 cells

ND7/23 cells (ECACC 92090903, RRID:CVCL_425, Merck, Darmstadt, Germany, cat. no. 92090903) were newly purchased and used until passage 20. The cell line is not listed in the International Cell Line Authentication Committee (ICLAC) database of cross-contaminated or misidentified cell lines. We did not perform further authentication of the cell line in the laboratory. Cells were cultured in Dulbecco's Modified Eagle's Medium (DMEM, Thermo Fisher Scientific, cat. no. 21010046) supplemented with 10% fetal calf serum (Pan Biotech, cat. no. P40-37500) and 0.1% penicillin/streptomycin (Thermo Fisher Scientific, cat. no. 15140122) at 37°C, 5% CO₂. 24 hr prior to transfection, cells were seeded onto 15 mm coverslips coated with collagen and poly-D-lysine. Cells were transfected using X-tremeGENE 9 (Sigma-Aldrich/ Merck, cat. no. 6365787001) at a ratio of 3:1 µl/µg DNA according to the manufacturer's protocol. Plasmids encoding PAC constructs and SthK-EGFP were used at a 3:1 ratio, and premixed before addition of the transfection reagent. Two days after transfection we performed whole-cell voltage clamp recordings on transfected cells identified by red fluorescence.

2.5 | Immunocytochemistry

At DIV 15–21, cultured neurons were fixed with 4% PFA in PBS for 10 min, then washed 3 times in PBS. Samples were permeabilized with 0.5% Triton-X100 for 5 min and blocked for 30 min in 2% normal goat serum in 0.1% Triton-X100. Samples were incubated with rabbit anti-RFP (against mKate2; 1:200; Thermo Fisher Scientific, cat. no. MA5-15257), mouse anti-microtubule-associated protein 2, clone 5F9 (MAP2; 1:100 Millipore/ Merck, cat. no. 05-346), and guinea pig anti-vesicular glutamate transporter 1 (VGLUT1; 1:4,000; Synaptic Systems, Göttingen, Germany, cat. no. 135304) primary antibodies at room temperature for 1.5 hr. Coverslips were washed 3 times with PBS before incubation with secondary antibodies conjugated with AlexaFluor-488, -555, or -647 (1:500; Invitrogen/ Thermo Fisher Scientific, cat. no. A11073, A27039, A27040) at room temperature for 1 hr. Finally, coverslips were washed 3 times with PBS and mounted in Mowiol (Carl Roth, Karlsruhe, Germany, cat. no. 0713.1).

2.6 | Confocal microscopy

Neurons were imaged on an upright TCS SP5 confocal microscope (Leica Microsystems, Wetzlar, Germany). The following laser lines were used to illuminate fluorescent specimens through a 63x oil immersion objective (1.4 NA): 488 nm (Argon laser), 568 nm (solid state), and 633 nm (Helium, Neon). Images of 1,024 × 1,024 pixels were acquired with 5x zoom at 400 Hz, with a 16x line average for the mKate2 signal. We quantified presynaptic enrichment of bPAC-constructs by calculating the ratio of the mKate2 signal in VGLUT1-positive spots (presynaptic terminals) and the mKate2 signal in VGLUT1-negative, but MAP2-positive areas (dendrites). For each cell, we created 4x4 pixel regions of interest (ROIs) on 20 VGLUT1-positive spots, and 20 ROIs on MAP2-positive, but VGLUT1-negative spots, using the Time Series Analyzer plugin (<https://imagej.nih.gov/ij/plugins/time-series.html>) in Fiji. For these ROIs, we measured the mean grey value in a single-plane confocal image of the mKate2 channel. After background subtraction, we then calculated the synapse to dendrite ratio of the averaged mKate2 signal in VGLUT1-positive spots to the averaged mKate2 signal in MAP2-positive spots.

2.7 | Electrophysiology of ND7/23 cells and neuronal cultures

Whole-cell voltage clamp recordings were performed on an IX73 inverted microscope (Olympus, Shinjuku, Tokyo, Japan) using a Multiclamp 700B amplifier under the control of a Digidata 1550 AD board and Clampex 10 software (all Molecular Devices). All recordings were performed at room temperature. Data were acquired at 10 kHz and filtered at 3 kHz. A TTL-controlled LED system (pE4000, CoolLED, Andover, UK) was coupled into the back port of the IX73

microscope by a single liquid light guide. Fluorescent light was passed through a quad band filter set (AHF, Tübingen, Germany, cat. no. F66-415) and an Olympus UPLSAPO 20 \times , NA 0.75 objective. For visualization of mKate2 fluorescence, we used a triple band filter set (AHF, cat. no. F66-502) with 575/25 nm excitation filter. Extracellular solution contained (in mM): 140 NaCl, 2.4 KCl, 10 HEPES, 10 glucose, 2 CaCl₂, and 4 MgCl₂ (pH adjusted to 7.3 with NaOH, 300 mOsm). The intracellular solution contained (in mM): 135 K-gluconate, 17.8 HEPES, 1 EGTA, 4.6 MgCl₂, 4 Na₂ATP, 0.3 NaGTP, 12 disodium phosphocreatine, and 50 U/ml creatine phosphokinase, pH adjusted to 7.3 with KOH, 300 mOsm. Unless otherwise stated, all chemicals were purchased from Tocris, Merck or Carl Roth.

ND7/23 cells co-expressing SthK-EGFP and synaptoPAC, mKate2-bPAC, or synaptophysin-mKate2 were voltage clamped at -60 mV. Photoactivated adenylyl cyclases were stimulated by 10 ms flashes of 474 nm light with varying intensity, which elicited cAMP-triggered K⁺ currents.

In whole-cell voltage clamp recordings from cultured neurons, membrane potential was set to -70 mV. Paired EPSCs were evoked every 5 s by triggering two unclamped action potentials at 25 Hz using 1 ms depolarizations of the soma to 0 mV. Granule cells were distinguished from other glutamatergic hippocampal neurons by their sensitivity of synaptic transmission to application of the group II metabotropic glutamate receptor agonist L-CCG I ((2S,1'S,2'S)-2-(Carboxycyclopropyl)glycines; 10 μ M; Tocris, Bristol, UK, cat. no. 0333). We classified neurons as granule cells if L-CCG I reduced their transmission by >55%, and neurons which showed <40% reduction of the EPSC as non-granule cells, while neurons with an intermediate effect on transmission were not included in further analysis (Figure 2a). The reduction of EPSC amplitudes by L-CCG I was calculated from the last four sweeps under L-CCG I and the last four sweeps from baseline before drug application. SynaptoPAC was activated by 12 flashes (1 s) of 474-nm light at 0.2 Hz at 70 mW mm⁻². The paired-pulse ratio was calculated as the ratio from the second and first EPSC amplitude with an interstimulus interval of 40 ms. Data were analyzed using AxoGraph X (AxoGraph, Sydney, Australia). EPSC potentiation and paired-pulse ratio changes by light stimulation or forskolin treatment were calculated from the average of 12 EPSCs during baseline and the last 6 EPSCs during the stimulation. For detection of miniature EPSCs, we filtered the recordings post hoc with a digital 1-kHz low-pass filter, and applied a template-based algorithm implemented in AxoGraph X. Frequency and amplitude of mEPSCs were corrected for false positives events, which we estimated by running the event detection with an inverted template (Rost et al., 2015). Recordings were excluded from the mEPSC analysis if false-positive events occurred at a frequency of >1 Hz.

2.8 | Stereotactic surgeries

Wild-type C57BL/6N mice (P25–P31; Charles River Strain Code 027) of both sexes were injected with 200 nl of AAV9.

hsyn:synaptophysin-mScarlet-bPAC using a NanoFil syringe with a 34-gauge needle (with UMP3 microinjection system and Micro4 controller; all from World Precision Instruments) at a rate of 40 nl/min. After the injection, the needle remained in position for another 5 min before it was slowly withdrawn. Mice were anesthetized under isoflurane (1.5% vol/vol in oxygen) during surgery and body temperature was maintained at 37°C. Animals received a subcutaneous injection of Carprofen (5 mg/kg) during the surgeries for analgesia. Injections were aimed at the following coordinates relative to bregma: anteroposterior (AP): 1.93 mm, mediolateral (ML): \pm 1.5 mm, dorsoventral (DV): -2.0 mm for the DG; AP: 1.75 mm, ML: 2.00 mm, DV: -2.1 mm for CA3. All animals were allowed to recover for at least 3 weeks before slice preparations and recording.

2.9 | Electrophysiology on hippocampal slices

Animals were anesthetized under isoflurane and decapitated. Under continuous safe light illumination, brains were quickly removed and placed in ice-cold sucrose-based artificial cerebrospinal fluid (sACSF) containing (in mM): 50 NaCl, 25 NaHCO₃, 10 glucose, 2.5 KCl, 7 MgCl₂, 1 NaH₂PO₄, 0.5 CaCl₂, and 150 sucrose, saturated with 95% O₂ and 5% CO₂. Tissue blocks containing the hippocampal formation were mounted on a vibratome (Leica VT 1200S, Leica Microsystems). Sagittal slices were cut at 300- μ m thickness and incubated in sucrose-based ACSF at 35°C for 30 min. Before the recording, slices were transferred into a submerged chamber filled with ACSF containing the following (in mM): 119 NaCl, 26 NaHCO₃, 10 glucose, 2.5 KCl, 1.3 MgCl₂, 1 NaH₂PO₄, and 2.5 CaCl₂, saturated with 95% O₂ and 5% CO₂. Slices were stored in ACSF for 0.5–6 hr at room temperature. A total of 34 mice were used for the slice experiments.

MF fEPSP recordings were performed at 21–24°C in a submerged recording chamber perfused with ACSF. Unless noted otherwise, MFs were stimulated at 0.05 Hz using a low-resistance glass electrode filled with ACSF, which was placed close to the internal side of granule cell layer of the dentate gyrus. The recording electrode filled with ACSF was placed in *stratum lucidum* of area CA3. The MF origin of fEPSPs was verified by the pronounced facilitation of synaptic response amplitudes upon 1 Hz stimulation or paired pulse stimulation at 25 Hz. In addition, we confirmed that fEPSPs were generated specifically by MFs by application of the type II metabotropic glutamate receptor agonist DCG IV ((2S,2'R,3'R)-2-(2',3'-dicarboxycyclopropyl)glycine; 1 μ M, Tocris, Bristol, UK, cat. no. 0975) at the end of each recording. DCG IV specifically suppresses transmitter release from MF terminals in CA3, but not from neighboring associational-commissural fiber synapses (Kamiya et al., 1996). Only responses that were inhibited by >80% were accepted as MF signals (16 slice excluded).

Recordings from Schaffer collateral synapses in CA1 were performed at 21–24°C in a submerged recording chamber perfused with ACSF at 2 ml/min. The stimulation electrode was placed in *stratum radiatum* proximal to the CA3 area and the recording electrode in the

stratum radiatum of CA1. Field EPSPs were stimulated at 0.05 Hz. A stable baseline of fEPSP amplitudes was recorded for at least 10 min before optical stimulation. In CA1 fEPSP recordings, we verified the fidelity of synaptic plasticity at the end of each recording (>30 min post optical stimulation) by electrically inducing LTP by four high frequency trains (100 pulses at 100 Hz, 10 s inter train interval). Only experiments in which we recorded >10% increase of the fEPSP 20–30 min after tetanic stimulation were included in the analysis (3 recordings excluded). As a measure for unstable stimulation conditions, we analyzed the magnitude of the presynaptic fiber volley and rejected recordings in which the fiber volley changed >10% over the course of the whole recording (1 recording excluded).

In both types of recordings, optical potentiation was induced by 10 pulses of blue light at 0.05 Hz from a 470 nm LED (pE300, CoolLED), which was passed through a 474/23 nm filter (AHF, cat. no. F39-474). Light was applied via an Olympus LUMPLFLN 40x (NA 0.8) water immersion objective, which was placed in *stratum lucidum* of CA3 for MF recordings and in *stratum radiatum* of CA1 for Schaffer collateral recordings. Data was acquired using a Multiclamp 700B amplifier, Digidata 1550A AD board, and Clampex 10.0 recording software (all Molecular Devices). In some recordings, data were acquired using a Multiclamp 700B amplifier, a BNC-2090 interface board with PCI 6035E A/D board (National Instruments) and IGOR Pro 6.12 as recording software (WaveMetrics, Lake Oswego, OR). Signals were sampled at 10 kHz and filtered at 3 kHz. Recordings were analyzed using Clampfit (Molecular Devices), IGOR Pro, or Axograph X.

2.10 | Statistics

No randomization or blinding was performed in the study. We did not perform a power analysis to determine sample size prior to the experiments, since the aim of our study was to establish a new technology without prior knowledge on effect size and variability. Statistical analyses were performed with GraphPad Prism 5.0 and 6.0 (Graphpad Software). Normality of data was assessed using D'Agostino-Pearson test and no test for outliers was conducted. Data are presented as mean \pm SD. N states the number of independent cell culture preparations or number of animals; and n states the number of cells recorded in cultures, or number of slices in fEPSP recordings.

3 | RESULTS

3.1 | SynaptoPAC design and functional validation

For the presynaptic targeting of bPAC we adopted a strategy previously established for optogenetic tools and fluorescent sensors (Granseth et al., 2006; Rost et al., 2015): By fusing bPAC together with a red fluorophore to the cytosolic C-terminus of the synaptic vesicle protein synaptophysin, we created synaptoPAC,

a presynaptically targeted version of bPAC (Figure 1a). When coexpressed with the cAMP-sensitive K⁺-channel SthK (Brams et al., 2014) in ND7/23 cells, light-activation of synaptoPAC triggered outward currents similar to untargeted bPAC, demonstrating efficient cAMP production by the enzyme (Figure 1b and c). No photocurrents were detected in cells co-expressing SthK and synaptophysin fused to mKate2 (Figure 1c). In cultures of rat hippocampal neurons, costainings for the glutamatergic vesicle marker VGLUT1 revealed a punctate expression of synaptoPAC, largely overlapping with VGLUT1 (Figure 1d), in contrast to a more diffuse expression pattern of the non-targeted bPAC-mKate2 (Figure 1e). We determined the synapse to dendrite ratio of the mKate2 signal from each cell as a measure of the relative presynaptic accumulation of the constructs (see Methods for details). The synapse to dendrite ratio was 2.9 ± 1.2 for synaptoPAC, but only 0.6 ± 0.5 for mKate2-bPAC, indicating a 4.8-fold enrichment of synaptoPAC at presynaptic terminals compared to untargeted bPAC (Figure 1f). Taken together, the fusion of bPAC to synaptophysin does not interfere with its enzymatic function and facilitates presynaptic accumulation of the construct.

Next, we wanted to test whether the presynaptically targeted, photoactivated adenylyl cyclase could enable light-triggered potentiation of transmitter release. In autaptic cultures of hippocampal granule cells stimulation of endogenous adenylyl cyclases by forskolin induces potentiation of transmitter release (Rost et al., 2010; Tong et al., 1996). We therefore chose this culture system as a test platform for establishing optogenetic potentiation of release by photocontrolled increase of presynaptic cAMP. We expressed synaptoPAC or synaptophysin-mKate2 as control in cultured hippocampal granule cells using lentivirus and performed whole-cell patch-clamp recordings 2–3 weeks post transduction. Hippocampal granule cells were identified by the specific suppression of their transmitter release by agonists of group II metabotropic glutamate receptors (Figure 2a, see Methods for details). Importantly, overexpression of neither synaptophysin-mKate2 nor synaptoPAC had any effect on excitatory postsynaptic currents (EPSCs), readily releasable pool, release probability, or short-term plasticity of transmitter release (Figure S1). After pharmacological characterization of the neuronal cell-type and recording a stable baseline of evoked transmission, we triggered synaptoPAC-mediated cAMP production with 12 1-s pulses of blue light at 0.2 Hz. Photostimulation increased EPSC amplitudes to $131 \pm 19\%$ of baseline in granule cells, but had no effect on transmission in non-granule cells (Figure 2b), indicating that the potentiation of synaptic transmission via photo-induced production of cAMP might be a cell-type-specific effect. We found no light-triggered potentiation in synaptophysin-expressing granule cells, which however, showed robust potentiation by forskolin (Figure S2a–c). In contrast, glutamatergic transmission of pyramidal neurons did not increase under forskolin (Figure 2c). In synaptoPAC-expressing granule cells, blue-light illumination occluded a further increase of EPSCs by forskolin (Figure 2c). Conversely, light-stimulation did not further increase EPSC amplitudes after forskolin treatment (Figure S2d–f). These findings indicate that both the pharmacologically as well as the

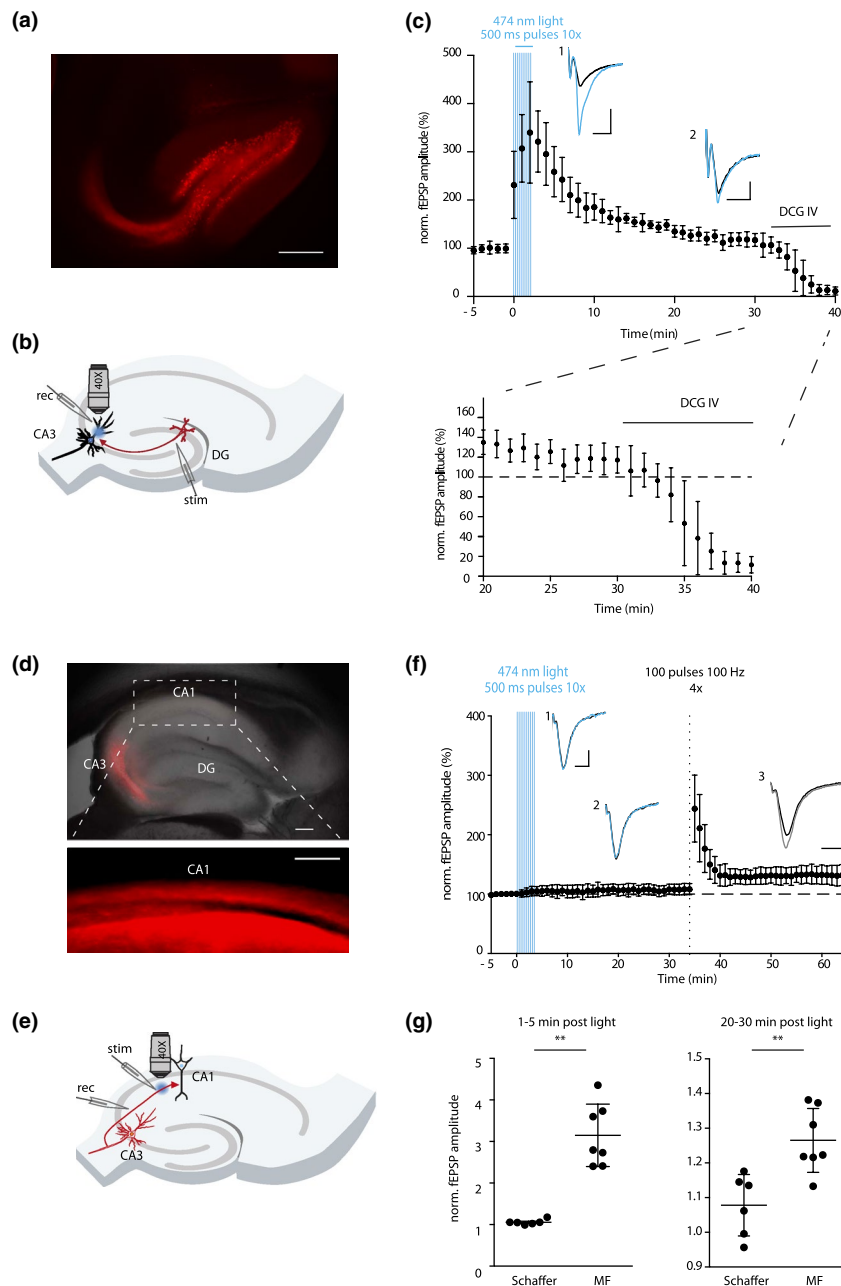


FIGURE 3 SynaptoPAC activation increases transmission at MF-CA3, but not at Schaffer collateral-CA1 synapses. (a) Fluorescent image of mScarlet confirming synaptoPAC expression in the dentate gyrus and MFs. Scale bar, 200 μ m. (b) Schematic illustration of the recording configuration in acute hippocampal slices for MF-CA3 synapses, with optical stimulation in *stratum lucidum* in CA3. (c) Optical activation with 500 ms pulses of 474 nm light (11 mW mm^{-2} , repeated 10 times at 0.05 Hz) acutely increased MF fEPSPs to $313 \pm 75\%$ of baseline, and triggered potentiation of MF fEPSPs ($126 \pm 9\%$) lasting >20 min. Example traces showing baseline synaptic transmission (black), (1) potentiated transmission in the first 5 min after illumination (blue; scale bar: 200 μ V, 20 ms), and (2) LTP after 20–30 min (scale bar: 100 μ V, 20 ms). Only experiments that showed $>80\%$ reduction of fEPSP amplitudes by application of DCG IV ($1 \mu\text{M}$) were considered as MF recordings ($n = 7$ slices, 6 mice). (d) Overlay of DIC and fluorescent image showing synaptoPAC expression in area CA3 and in Schaffer collaterals (inset). Scale bars: 200 μ m. (e) Scheme of the recording configuration at Schaffer collateral-CA1 synapses. (f) In Schaffer collateral synapses expressing synaptoPAC, blue light stimulation had no immediate effect in the first 5 min post illumination (1) ($104 \pm 6\%$ of baseline), nor did it cause strong LTP after 20–30 min (2) ($107 \pm 8\%$). However, these synapses showed post-tetanic potentiation of $192 \pm 42\%$ and long-term potentiation (3) ($132 \pm 15\%$) following 4 trains of 100 electrical stimuli at 100 Hz ($n = 6$ slices, 3 mice). Scale bars: 100 μ V, 10 ms. (g) Direct comparison of the synaptoPAC effect on transmission at MF-CA3 and CA3-CA1 synapses. In both cases the effect size induced by synaptoPAC is significantly higher in MF synapses compared to Schaffer collaterals synapses (1–5 min: $p = .0006$; 20–30 min: $p = .02$, both Mann-Whitney test). Data points shown in (c) and (f) are binned to 1 min.



optogenetically driven increase of cAMP saturate the downstream signaling cascade for presynaptic potentiation in granule cells. The optogenetic potentiation also altered the short-term plasticity of synaptic transmission, by reducing the amplitude ratio of two EPSCs evoked at 25 Hz (Figure 2d). This decrease in paired-pulse ratio (PPR) indicates a presynaptic origin of the effect, and often correlates with an increase in the release probability (Abbott & Regehr, 2004; Zucker & Regehr, 2002). In contrast, synaptoPAC activation did not alter the PPR in non-granule cells. Of note, light-triggered elevation of presynaptic cAMP increased the frequency of miniature EPSCs (mEPSCs), but did not affect mEPSC amplitudes, independent of the cell type (Figure S3). In summary, our experiments in neuronal cultures indicate that synaptoPAC acts via a presynaptic mechanism and increases evoked release in a cell-type-specific manner.

3.2 | SynaptoPAC potentiates transmission at MF-CA3 synapses

Next, we tested whether synaptoPAC was able to potentiate transmission at hippocampal MF-CA3 synapses, the classical preparation to study presynaptic forms of LTP. We injected AAVs encoding synaptoPAC into the dentate gyrus of wildtype mice *in vivo*. After three to four weeks, we prepared acute hippocampal slices, and found strong synaptoPAC expression in dentate gyrus granule cells and the MF tract (Figure 3a). We electrically stimulated MF transmission and recorded field excitatory postsynaptic potentials (fEPSPs) in area CA3. SynaptoPAC was activated by applying blue light pulses locally at MF terminals through a 40x objective in the area of the recording electrode (Figure 3b). During an initial screening (Figure S3a and b) we tested several activation protocols for synaptoPAC and found robust potentiation with 10 pulses of 474 nm light, 11 mW mm⁻², applied at 0.05 Hz, with 0.5 s pulse duration (total light dosage: 55 mW mm⁻²). MF fEPSP amplitudes increased to 313 ± 75% within 5 min after the start of the optical induction protocol (Figure 3c). Subsequently, fEPSPs decreased but were still potentiated by 126 ± 9% after 20–30 min post induction. In a separate set of experiments we found that a 10x lower light dosage (5.5 mW s mm⁻²) was equally effective for stimulating synaptic potentiation (Figure S4; post-light potentiation: 363 ± 57%, potentiation after 20–30 min: 130 ± 6.5%), indicating that a wide range of light intensities is suitable for the activation of synaptoPAC. At the end of each recording we verified the MF origin of the signal by applying the metabotropic glutamate receptor agonist DCG-IV (Figure 3c), which specifically suppresses release from MF terminals, but not from neighboring associational-commissural fiber synapses in CA3 (Kamiya et al., 1996). Next, we examined whether synaptoPAC-induced plasticity was specific for synapses that express cAMP-dependent presynaptic LTP. For this we expressed synaptoPAC in CA3 pyramidal neurons (Figure 3d and e), and recorded fEPSPs from Schaffer collateral synapses in CA1, which express an NMDA (N-methyl-D-aspartate) receptor-dependent, postsynaptic form of LTP (Herring & Nicoll, 2016). Activation of synaptoPAC with

the same light pulse protocol (total light dosage: 55 mW s mm⁻²) that elicited strong potentiation in MF-CA3 synapses did not induce significant potentiation on Schaffer collateral synapses (Figure 3f and g), however, these synapses showed potentiation following tetanic electrical stimulation (Figure 3f). Together, the experiments in acute hippocampal slices confirm a synapse-specific effect of synaptoPAC.

3.3 | SynaptoPAC activation alters presynaptic release probability

One of the distinguishing characteristics of MF-CA3 synapses is the pronounced short-term facilitation of synaptic transmission upon repetitive activation (Nicoll & Schmitz, 2005). Presynaptic LTP at MF-CA3 synapses reduces the dynamic range of the short-term plasticity of release (Gundlfinger et al., 2007; Weisskopf et al., 1994; Zalutsky & Nicoll, 1990). To test whether optogenetic potentiation similarly alters MF release properties, we tested short-term plasticity of MF fEPSPs using two different protocols: 5 pulses at 25 Hz and 20 pulses at 1 Hz, both before and after blue-light stimulation (Figure 4a). Indeed, illumination significantly decreased both the PPR of the second to the first and of the fifth to the first fEPSP in the 25 Hz burst (Figure 4b). Optogenetic potentiation also caused a significant decrease of the frequency facilitation that is observed when increasing stimulation frequency from 0.05 Hz to 1 Hz (Figure 4c). Both test protocols indicate that synaptoPAC-driven MF potentiation changes the release probability. Control recordings of MF fEPSPs in hippocampal slices from non-injected wildtype mice demonstrated that the dynamics of short-term plasticity of MF transmission were not decreasing when tested repetitively (Figure S5a and b). Of note, the 1 Hz frequency facilitation in slices from non-infected control animals was similar to that observed in slices from synaptoPAC-expressing animals (control: 4.3 ± 1.2, synaptoPAC: 4.4 ± 2.3), indicating that overexpression of synaptoPAC itself did not alter MF release properties. In a subset of recordings, we also applied forskolin, which triggered a 2.4 ± 1 fold increase in fEPSP amplitude, and in turn significantly reduced both frequency facilitation and paired-pulse facilitation (Figure S5c–e), confirming previous reports (Huang et al., 1994; Weisskopf et al., 1994). Taken together, synaptoPAC enables light-controlled production of cAMP at presynaptic terminals, which leads to an increase in transmitter release specifically at synapses sensitive to cAMP.

4 | DISCUSSION

Tools enabling selective and remote-controlled induction of presynaptic plasticity are required to elucidate the mechanisms and functional relevance of presynaptic LTP (Monday et al., 2018). SynaptoPAC, a fusion of the photoactivated adenylyl cyclase bPAC to the synaptic vesicle protein synaptophysin, is well suited for such investigations: We demonstrate that overexpression of synaptoPAC does not affect synaptic transmission, and that the optogenetic

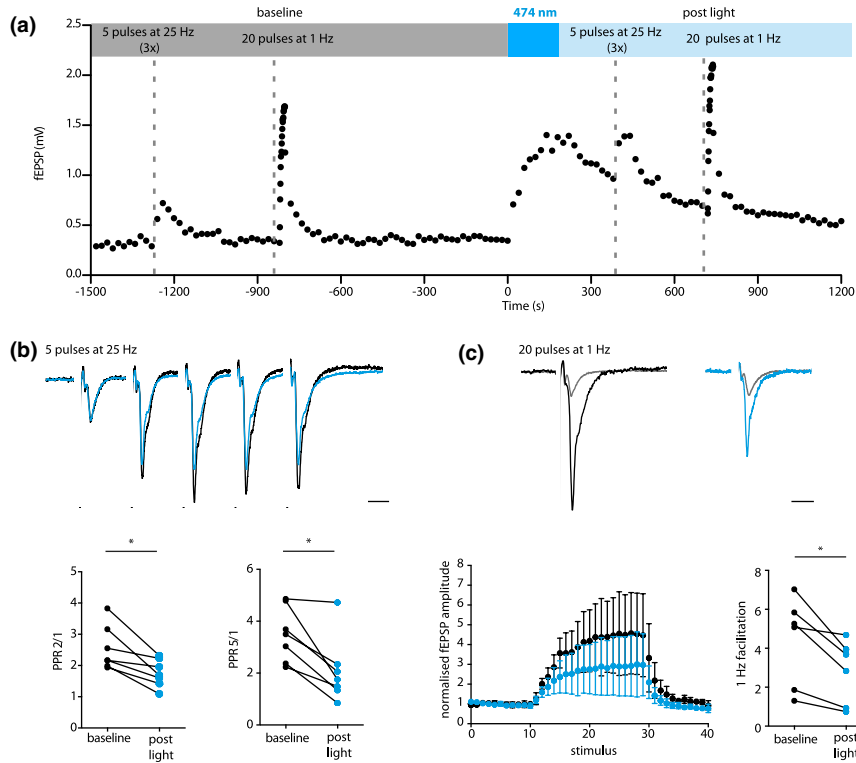


FIGURE 4 SynaptoPAC mediates potentiation by a presynaptic mechanism. (a) Typical representation of the recording protocol for MF short-term plasticity: MF were first stimulated electrically with 5 pulses at 25 Hz and with 20 pulses at 1 Hz. Following synaptoPAC activation by 10 pulses of 474 nm light (500 ms, 11 mW mm⁻², 0.2 Hz), the 25 Hz and 1 Hz stimulus trains were applied again 5 and 10 min after optical induction, respectively. For the 25 Hz trains, only the first fEPSP amplitude was plotted. (b) Representative traces of five MF fEPSP elicited at 25 Hz before (black) and after light stimulation (blue), scaled to the amplitude of the first fEPSP. Scale bar: 20 ms. SynaptoPAC induced potentiation significantly decreased the paired-pulse ratio between the second and the first fEPSPs (baseline: 2.54 ± 0.7 , post light: 1.76 ± 0.43 ; $n = 7$ slices, 6 mice; $p = .02$, Wilcoxon signed-rank test), and the fifth and first fEPSPs (baseline: 3.50 ± 1.05 , post light: 2.08 ± 1.26 ; $p = .02$, Wilcoxon signed-rank test). (c) Traces showing the first and last MF fEPSP evoked by a train of 20 stimuli applied at 1 Hz before (black) and after (blue) blue-light illumination. Traces are normalized to the first fEPSP in the train. Scale bar: 20 ms. 1 Hz facilitation was significantly decreased after optogenetic potentiation (baseline: 4.40 ± 2.29 , post light: 2.80 ± 1.64 ; $n = 7$ slices, 6 mice; $p = .03$, Wilcoxon signed-rank test).

production of cAMP is equally effective as pharmacological activation of endogenous adenylyl cyclases. Because of its small size, the construct is easily expressed *in vivo* via AAVs, which will allow for cell-type-specific expression through the use of Cre-lox recombination or cell-type-specific promoters. The highly light sensitive bPAC used in the synaptoPAC construct is selectively activated by blue light (Stierl et al., 2011), which enables experimental combinations with other optogenetic actuators and fluorescent sensors sensitive to light >520 nm (Bernal Sierra et al., 2018). A previous study in hippocampal pyramids revealed a stronger increase in cAMP levels by bPAC activation than by forskolin application, probably because of the limited capacity of the endogenous adenylyl cyclases activated by forskolin, which are bypassed by the photoactivated adenylyl cyclases (Stierl et al., 2011). However, this study analyzed cAMP-gated currents from overexpressed cyclic-nucleotide-gated channels, which are likely not saturated by endogenously produced cAMP. In our recordings from autaptic granule cells we found mutual occlusion of both forskolin- and synaptoPAC-induced potentiation of transmission, indicating that both manipulations saturate the signaling

cascade downstream of cAMP (Figure 2c, Figure S2). In extracellular field recordings from MFs the post-light potentiation following synaptoPAC activation was higher than forskolin-induced potentiation, but not statistically different (synaptoPAC (Figure 3c): $313 \pm 75\%$; forskolin (Figure S5e): $240 \pm 97\%$; $p = .13$, Mann-Whitney *U* test). Importantly, we show that local illumination of axonal terminals is sufficient to trigger potentiation, allowing target area-specific manipulations. In summary, our results suggest that synaptoPAC is at least as effective as the classical pharmacological induction of presynaptic LTP by forskolin, with the advantage that the manipulation by optogenetic stimulation is clearly confined to the presynaptic compartment.

Interestingly, the time course of synaptoPAC-mediated potentiation of MF transmission in hippocampal slices (Figure 3c, Figure S4c) matches the time course of post-tetanic potentiation induced by electrical stimulation with regular high frequency trains or naturally occurring activity patterns (Gundfänger et al., 2010; Vandael et al., 2020), with a strong initial increase that decays with a tau of approx. 20 min. Our data demonstrate



that at MF terminals a transient increase of presynaptic cAMP in the absence of high-frequency action potential firing is sufficient for synaptic potentiation, in contrast to CA3-CA1 synapses, where a selective increase of presynaptic cAMP by synaptoPAC is not sufficient to potentiate action potential-evoked transmission (Figure 3). Previously, forskolin in combination with phosphodiesterase inhibitors was used to increase transmission at CA3-CA1 synapses (Chavez-Noriega & Stevens, 1992, 1994; Frerking et al., 2001; Otmakhov et al., 2004). However, it is unclear whether this form of chemical potentiation is purely presynaptic, if physiological activity can recapitulate the pharmacological stimulation, and to which extent cAMP-independent effects of forskolin contribute to it (Laurenza et al., 1989). In our hands, a selective increase of presynaptic cAMP by optogenetic means without pharmacological inhibition of phosphodiesterases did not induce strong potentiation at Schaffer collateral synapses nor in cultures of hippocampal non-granule cells. Our findings suggest that Schaffer collateral synapses not just lack presynaptic adenylyl cyclases but differ in key features of the molecular machinery required for presynaptic long-term plasticity, resulting in a synapse-specific effect of cAMP on evoked transmission. Of note, and in line with previous reports (Maximov et al., 2007; Steuer Costa et al., 2017), synaptoPAC-driven elevation of presynaptic cAMP increased mEPSC frequency, irrespective of the glutamatergic cell type. Presynaptic cAMP promotes synapsin phosphorylation by PKA, causing dissociation of synapsin from vesicles, and spatial reorganization of vesicles in the terminal (Menegon et al., 2006; Patzke et al., 2019; Vaden et al., 2019). In future, optogenetic control of presynaptic cAMP by synaptoPAC will provide novel avenues to study such kinds of vesicle pool regulation.

SynaptoPAC-driven enhancement of release will be useful to study computational aspects of presynaptic potentiation, which alters short-term synaptic filtering dynamics by shifting spike transmission from a high-pass toward a low-pass mode (Abbott & Regehr, 2004). How this altered synaptic computation affects encoding, storage and recall of associative memories is mostly unknown (Rebola et al., 2017). So far, causative behavioral studies have relied on either genetic ablation of major presynaptic molecules, or drugs of abuse acting on presynaptic metabotropic receptors such as cannabinoids, opioids, and cocaine (for review see Kauer & Malenka, 2007; Monday et al., 2018). However, genetic deletions act on very long time scales, and both genetic and pharmacological manipulations may have systemic effects. It is therefore difficult to unambiguously relate these interventions to synaptic alterations and behavioral consequences. Presynaptic plasticity has also been associated with pathophysiological brain conditions such as schizophrenia, autism spectrum disorders, and addiction, but it remains unclear whether aberrant presynaptic plasticity contributes causally or results from the disease (Monday & Castillo, 2017). We expect that synaptoPAC represents a versatile optogenetic tool to unravel some of the outstanding questions of presynaptic plasticity, both under physiological and pathophysiological conditions.

5 | COMPETING INTERESTS

The authors declare no competing interests. AAV expression vectors for synaptoPAC are available on Addgene.org (plasmid #153100 and #153085).

ACKNOWLEDGMENTS

The authors thank Katja Pötschke, Bettina Brokowski, Anke Schönherr, Susanne Rieckmann and Katja Czeselsky for excellent technical assistance, and Felicitas Brüntgens for help with the neuronal cell culture. The authors thank Rosanna Sammons for comments on the manuscript. This work was supported by grants from the Deutsche Forschungsgemeinschaft (DFG; German Research Foundation) under Germany's Excellence Strategy – EXC-2049 – 390688087 to D.S. and C.R., SPP 1926 (B.R.R.), SPP 1665 (D.S.), SFB 1315 (D.S.), SFB 958 (C.R., D.S.). The plasmid encoding bPAC was kindly provided by the laboratory of Peter Hegemann, Humboldt University Berlin, Germany. SthK-EGFP was kindly provided by Franziska Schneider-Warme, Institute for Experimental Cardiovascular Medicine, University of Freiburg, Germany. A previous version of this manuscript was posted on bioRxiv (www.biorxiv.org/content/10.1101/2020.03.27.011635v1).

Open access funding enabled and organized by ProjektDEAL.

All experiments were conducted in compliance with the ARRIVE guidelines.

AUTHORS' CONTRIBUTIONS

S.O., L.M.-V., L.F., A.S., and B.R.R. performed the experiments. S.O., L.F., and B.R.R. analyzed the data. B.R.R. designed the tool, and B.R.R., D.S., and C.R. conceptualized the research. B.R.R. and D.S. acquired funding for the project and supervised the work. B.R.R. and S.O. wrote the paper with input from all authors. All authors approved submission of the manuscript.

OPEN RESEARCH BADGES



This article has received a badge for *Open Materials* because it provided all relevant information to reproduce the study in the manuscript. More information about the Open Science badges can be found at pAAV-syn-synaptoPAC-minWPRE: <https://www.addgene.org/153085/> and pAAV-syn-FLEX-synaptoPAC-minWPRE: <https://www.addgene.org/153100/>

ORCID

Silvia Oldani <https://orcid.org/0000-0002-9034-6237>

Laura Moreno-Velasquez <https://orcid.org/0000-0001-9735-0039>

Lukas Faiss

<https://orcid.org/0000-0001-5150-5541>

Alexander Stumpf <https://orcid.org/0000-0002-1510-6970>

Christian Rosenmund <https://orcid.org/0000-0002-3905-2444>

Dietmar Schmitz <https://orcid.org/0000-0003-2741-5241>

Benjamin R. Rost <https://orcid.org/0000-0003-1906-0081>



REFERENCES

- Abbott, L. F., & Regehr, W. G. (2004). Synaptic computation. *Nature*, *431*, 796–803. <https://doi.org/10.1038/nature03010>
- Bernal Sierra, Y. A., Rost, B. R., Pofahl, M., Fernandes, A. M., Kopton, R. A., Moser, S., Holtkamp, D., Masala, N., Beed, P., Tukker, J. J., Oldani, S., Bönigk, W., Kohl, P., Baier, H., Schneider-Warme, F., Hegemann, P., Beck, H., Seifert, R., & Schmitz, D. (2018). Potassium channel-based optogenetic silencing. *Nature Communications*, *9*, 4611. <https://doi.org/10.1038/s41467-018-07038-8>
- Brams, M., Kusch, J., Spurny, R., Benndorf, K., & Ulens, C. (2014). Family of prokaryote cyclic nucleotide-modulated ion channels. *Proceedings of the National Academy of Sciences*, *111*, 7855–7860. <https://doi.org/10.1073/pnas.1401917111>
- Castillo, P. E. (2012). Presynaptic LTP and LTD of excitatory and inhibitory synapses. *Cold Spring Harbor Perspectives in Biology*, *4*, a005728–a005728. <https://doi.org/10.1101/cshperspect.a005728>
- Castillo, P. E., Janz, R., Sudhof, T. C., Tzounopoulos, T., Malenka, R. C., & Nicoll, R. A. (1997). Rab3A is essential for mossy fibre long-term potentiation in the hippocampus. *Nature*, *388*, 590–593. <https://doi.org/10.1038/41574>
- Castillo, P. E., Schoch, S., Schmitz, F., Sudhof, T. C., & Malenka, R. C. (2002). RIM1alpha is required for presynaptic long-term potentiation. *Nature*, *415*, 327–330.
- Castro-Alamancos, M. A., & Calcagnotto, M. E. (1999). Presynaptic long-term potentiation in corticothalamic synapses. *Journal of Neuroscience*, *19*, 9090–9097. <https://doi.org/10.1523/JNEUROSCI.19-20-09090.1999>
- Chavez-Noriega, L. E., & Stevens, C. F. (1992). Modulation of synaptic efficacy in field CA1 of the rat hippocampus by forskolin. *Brain Research*, *574*, 85–92. [https://doi.org/10.1016/0006-8993\(92\)90803-H](https://doi.org/10.1016/0006-8993(92)90803-H)
- Chavez-Noriega, L. E., & Stevens, C. F. (1994). Increased transmitter release at excitatory synapses produced by direct activation of adenylate cyclase in rat hippocampal slices. *Journal of Neuroscience*, *14*, 310–317. <https://doi.org/10.1523/JNEUROSCI.14-01-00310.1994>
- Ferguson, G. D., & Storm, D. R. (2004). Why calcium-stimulated adenyl cyclases? *Physiology (Bethesda)*, *19*, 271–276. <https://doi.org/10.1152/physiol.00010.2004>
- Fernandes, H. B., Riordan, S., Nomura, T., Remmers, C. L., Kraniotis, S., Marshall, J. J., Kukreja, L., Vassar, R., & Contractor, A. (2015). Epac2 mediates cAMP-dependent potentiation of neurotransmission in the hippocampus. *Journal of Neuroscience*, *35*, 6544–6553. <https://doi.org/10.1523/JNEUROSCI.0314-14.2015>
- Fourcaudot, E., Gambino, F., Humeau, Y., Casassus, G., Shaban, H., Poulain, B., & Luthi, A. (2008). cAMP/PKA signaling and RIM1alpha mediate presynaptic LTP in the lateral amygdala. *Proceedings of the National Academy of Sciences of the United States of America*, *105*, 15130–15135.
- Frerking, M., Schmitz, D., Zhou, Q., Johansen, J., & Nicoll, R. A. (2001). Kainate receptors depress excitatory synaptic transmission at CA3–CA1 synapses in the hippocampus via a direct presynaptic action. *Journal of Neuroscience*, *21*, 2958–2966.
- Granseth, B., Odermatt, B., Royle, S. J., & Lagnado, L. (2006). Clathrin-mediated endocytosis is the dominant mechanism of vesicle retrieval at hippocampal synapses. *Neuron*, *51*, 773–786. <https://doi.org/10.1016/j.neuron.2006.08.029>
- Gundlfinger, A., Breustedt, J., Sullivan, D., & Schmitz, D. (2010). Natural spike trains trigger short- and long-lasting dynamics at hippocampal mossy fiber synapses in rodents. *PLoS One*, *5*, e9961. <https://doi.org/10.1371/journal.pone.0009961>
- Gundlfinger, A., Leibold, C., Gebert, K., Moisel, M., Schmitz, D., & Kempter, R. (2007). Differential modulation of short-term synaptic dynamics by long-term potentiation at mouse hippocampal mossy fibre synapses. *Journal of Physiology*, *585*, 853–865. <https://doi.org/10.1113/jphysiol.2007.143925>
- Hashimoto-dani, Y., Nasrallah, K., Jensen, K. R., Chavez, A. E., Carrera, D., & Castillo, P. E. (2017). LTP at hilar mossy cell-dentate granule cell synapses modulates dentate gyrus output by increasing excitation/inhibition balance. *Neuron*, *95*(928–943), e923. <https://doi.org/10.1016/j.neuron.2017.07.028>
- Herring, B. E., & Nicoll, R. A. (2016). Long-term potentiation: From CaMKII to AMPA receptor trafficking. *Annual Review of Physiology*, *78*, 351–365. <https://doi.org/10.1146/annurev-physiol-021014-071753>
- Huang, Y. Y., & Kandel, E. R. (1998). Postsynaptic induction and PKA-dependent expression of LTP in the lateral amygdala. *Neuron*, *21*, 169–178. [https://doi.org/10.1016/S0896-6273\(00\)80524-3](https://doi.org/10.1016/S0896-6273(00)80524-3)
- Huang, Y. Y., Li, X. C., & Kandel, E. R. (1994). cAMP contributes to mossy fiber LTP by initiating both a covalently mediated early phase and macromolecular synthesis-dependent late phase. *Cell*, *79*, 69–79. [https://doi.org/10.1016/0092-8674\(94\)90401-4](https://doi.org/10.1016/0092-8674(94)90401-4)
- Kaesler-Woo, Y. J., Younts, T. J., Yang, X., Zhou, P., Wu, D., Castillo, P. E., & Sudhof, T. C. (2013). Synaptotagmin-12 phosphorylation by cAMP-dependent protein kinase is essential for hippocampal mossy fiber LTP. *Journal of Neuroscience*, *33*, 9769–9780. <https://doi.org/10.1523/JNEUROSCI.5814-12.2013>
- Kamiya, H., Shinozaki, H., & Yamamoto, C. (1996). Activation of metabotropic glutamate receptor type 2/3 suppresses transmission at rat hippocampal mossy fibre synapses. *Journal of Physiology*, *493*(Pt 2), 447–455. <https://doi.org/10.1113/jphysiol.1996.sp021395>
- Kauer, J. A., & Malenka, R. C. (2007). Synaptic plasticity and addiction. *Nature Reviews Neuroscience*, *8*, 844–858. <https://doi.org/10.1038/nrn2234>
- Lachamp, P. M., Liu, Y., & Liu, S. J. (2009). Glutamatergic modulation of cerebellar interneuron activity is mediated by an enhancement of GABA release and requires protein kinase A/RIM1alpha signaling. *Journal of Neuroscience*, *29*, 381–392.
- Laurenza, A., Sutkowski, E. M., & Seamon, K. B. (1989). Forskolin: A specific stimulator of adenyl cyclase or a diterpene with multiple sites of action? *Trends in Pharmacological Sciences*, *10*, 442–447. [https://doi.org/10.1016/S0165-6147\(89\)80008-2](https://doi.org/10.1016/S0165-6147(89)80008-2)
- Maximov, A., Shin, O. H., Liu, X., & Sudhof, T. C. (2007). Synaptotagmin-12, a synaptic vesicle phosphoprotein that modulates spontaneous neurotransmitter release. *Journal of Cell Biology*, *176*, 113–124. <https://doi.org/10.1083/jcb.200607021>
- Menegon, A., Bonanomi, D., Albertinazzi, C., Lotti, F., Ferrari, G., Kao, H. T., Benfenati, F., Baldelli, P., & Valtorta, F. (2006). Protein kinase A-mediated synapsin I phosphorylation is a central modulator of Ca²⁺-dependent synaptic activity. *Journal of Neuroscience*, *26*, 11670–11681. <https://doi.org/10.1523/JNEUROSCI.3321-06.2006>
- Monday, H. R., & Castillo, P. E. (2017). Closing the gap: Long-term presynaptic plasticity in brain function and disease. *Current Opinion in Neurobiology*, *45*, 106–112. <https://doi.org/10.1016/j.conb.2017.05.011>
- Monday, H. R., Younts, T. J., & Castillo, P. E. (2018). Long-term plasticity of neurotransmitter release: Emerging mechanisms and contributions to brain function and disease. *Annual Review of Neuroscience*, *41*, 299–322. <https://doi.org/10.1146/annurev-neuro-080317-062155>
- Nicoll, R. A., & Schmitz, D. (2005). Synaptic plasticity at hippocampal mossy fibre synapses. *Nature Reviews Neuroscience*, *6*, 863–876. <https://doi.org/10.1038/nrn1786>
- Otmakhov, N., Khibnik, L., Otmakhova, N., Carpenter, S., Riahi, S., Asrican, B., & Lisman, J. (2004). Forskolin-induced LTP in the CA1 hippocampal region is NMDA receptor dependent. *Journal of Neurophysiology*, *91*, 1955–1962. <https://doi.org/10.1152/jn.00941.2003>
- Patzke, C., Brockmann, M. M., Dai, J., Gan, K. J., Grauel, M. K., Fenske, P., Liu, Y. U., Acuna, C., Rosenmund, C., & Südhof, T. C. (2019). Neuromodulator signaling bidirectionally controls vesicle numbers in human synapses. *Cell*, *179*(498–513), e422. <https://doi.org/10.1016/j.cell.2019.09.011>

- Rebola, N., Carta, M., & Mulle, C. (2017). Operation and plasticity of hippocampal CA3 circuits: Implications for memory encoding. *Nature Reviews Neuroscience*, *18*, 208–220. <https://doi.org/10.1038/nrn.2017.10>
- Rost, B. R., Breustedt, J., Schoenherr, A., Grosse, G., Ahnert-Hilger, G., & Schmitz, D. (2010). Autaptic cultures of single hippocampal granule cells of mice and rats. *European Journal of Neuroscience*, *32*, 939–947. <https://doi.org/10.1111/j.1460-9568.2010.07387.x>
- Rost, B. R., Schneider, F., Grauel, M. K., Wozny, C., G Bentz, C., Blessing, A., Rosenmund, T., Jentsch, T. J., Schmitz, D., Hegemann, P., & Rosenmund, C. (2015). Optogenetic acidification of synaptic vesicles and lysosomes. *Nature Neuroscience*, *18*, 1845–1852. <https://doi.org/10.1038/nn.4161>
- Rost, B. R., Schneider-Warme, F., Schmitz, D., & Hegemann, P. (2017). Optogenetic tools for subcellular applications in neuroscience. *Neuron*, *96*, 572–603. <https://doi.org/10.1016/j.neuron.2017.09.047>
- Salin, P. A., Malenka, R. C., & Nicoll, R. A. (1996). Cyclic AMP mediates a presynaptic form of LTP at cerebellar parallel fiber synapses. *Neuron*, *16*, 797–803. [https://doi.org/10.1016/S0896-6273\(00\)80099-9](https://doi.org/10.1016/S0896-6273(00)80099-9)
- Steuer Costa, W., Yu, S. C., Liewald, J. F., & Gottschalk, A. (2017). Fast cAMP modulation of neurotransmission via neuropeptide signals and vesicle loading. *Current Biology*, *27*, 495–507. <https://doi.org/10.1016/j.cub.2016.12.055>
- Stierl, M., Stumpf, P., Udvari, D. et al (2011). Light modulation of cellular cAMP by a small bacterial photoactivated adenylyl cyclase, bPAC, of the soil bacterium *Beggiatoa*. *Journal of Biological Chemistry*, *286*, 1181–1188.
- Takeuchi, T., Duszkievicz, A. J., & Morris, R. G. (2014). The synaptic plasticity and memory hypothesis: Encoding, storage and persistence. *Philosophical Transactions of the Royal Society of London. Series B, Biological Sciences*, *369*, 20130288. <https://doi.org/10.1098/rstb.2013.0288>
- Tong, G., Malenka, R. C., & Nicoll, R. A. (1996). Long-term potentiation in cultures of single hippocampal granule cells: A presynaptic form of plasticity. *Neuron*, *16*, 1147–1157. [https://doi.org/10.1016/S0896-6273\(00\)80141-5](https://doi.org/10.1016/S0896-6273(00)80141-5)
- Vaden, J. H., Banumurthy, G., Gusarevich, E. S., Overstreet-Wadiche, L., & Wadiche, J. I. (2019). The readily-releasable pool dynamically regulates multivesicular release. *Elife*, *8*. <https://doi.org/10.7554/eLife.47434>
- Vandael, D., Borges-Merjane, C., Zhang, X., & Jonas, P. (2020). Short-term plasticity at hippocampal mossy fiber synapses is induced by natural activity patterns and associated with vesicle pool engram formation. *Neuron*, *107*(509–521), e507. <https://doi.org/10.1016/j.neuron.2020.05.013>
- Weisskopf, M. G., Castillo, P. E., Zalutsky, R. A., & Nicoll, R. A. (1994). Mediation of hippocampal mossy fiber long-term potentiation by cyclic AMP. *Science*, *265*, 1878–1882. <https://doi.org/10.1126/science.7916482>
- Wozny, C., Maier, N., Fidzinski, P., Breustedt, J., Behr, J., & Schmitz, D. (2008). Differential cAMP signaling at hippocampal output synapses. *Journal of Neuroscience*, *28*, 14358–14362. <https://doi.org/10.1523/JNEUROSCI.4973-08.2008>
- Yang, Y., & Calakos, N. (2011). Munc13-1 is required for presynaptic long-term potentiation. *Journal of Neuroscience*, *31*, 12053–12057. <https://doi.org/10.1523/JNEUROSCI.2276-11.2011>
- Zalutsky, R. A., & Nicoll, R. A. (1990). Comparison of two forms of long-term potentiation in single hippocampal neurons. *Science*, *248*, 1619–1624. <https://doi.org/10.1126/science.2114039>
- Zucker, R. S., & Regehr, W. G. (2002). Short-term synaptic plasticity. *Annual Review of Physiology*, *64*, 355–405. <https://doi.org/10.1146/annurev.physiol.64.092501.114547>

SUPPORTING INFORMATION

Additional supporting information may be found online in the Supporting Information section.

How to cite this article: Oldani S, Moreno-Velasquez L, Faiss L, et al. SynaptoPAC, an optogenetic tool for induction of presynaptic plasticity. *J Neurochem*. 2020;00:1–13. <https://doi.org/10.1111/jnc.15210>

SynaptoPAC, an Optogenetic Tool for Induction of Presynaptic Plasticity

- Supplementary information -

Silvia Oldani^{1,2}, Laura Moreno-Velasquez², Lukas Faiss^{1,2}, Alexander Stumpf², Christian Rosenmund², Dietmar Schmitz^{1-5,*}, Benjamin R. Rost^{1,*}

¹ German Center for Neurodegenerative Diseases (DZNE), 10117 Berlin, Germany

² Charité – Universitätsmedizin Berlin, corporate member of Freie Universität Berlin and Humboldt-Universität zu Berlin, and Berlin Institute of Health, NeuroCure Cluster of Excellence, Charitéplatz 1, 10117 Berlin, Germany

³ Max-Delbrück-Centrum (MDC) for Molecular Medicine in the Helmholtz Association, 13125 Berlin, Germany.

⁴ Bernstein Center for Computational Neuroscience, 10115 Berlin, Germany.

⁵ Einstein Center for Neurosciences Berlin, 10117 Berlin, Germany.

* Correspondence: benjamin.rost@dzne.de; dietmar.schmitz@charite.de

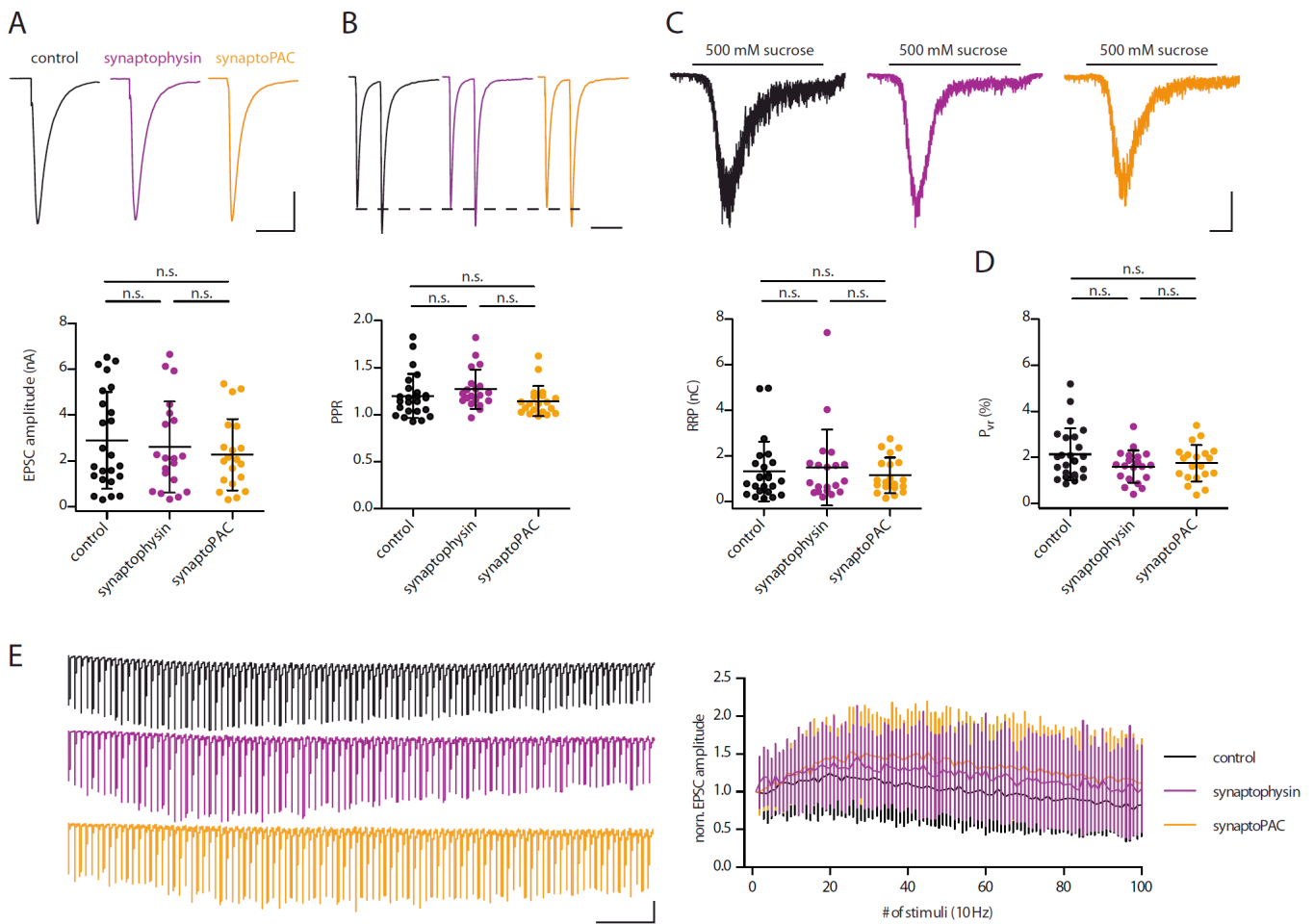


Figure S1. Overexpression of synaptophysin-mKate2 or synaptoPAC does not affect synaptic transmitter release in autaptic cultures of hippocampal granule cells.

(A) EPSCs recorded from uninfected granule cells (control) and granule cells overexpressing synaptophysin-mKate2 and synaptoPAC. Scale bars: 1 nA, 20 ms. Average EPSC amplitudes were not significantly different between the three groups (control: 2.9 ± 2.1 nA; synaptophysin: 2.6 ± 2.0 nA; synaptoPAC: 2.3 ± 1.6 nA). **(B)** Pairs of EPSCs evoked at 40 ms inter-stimulus interval showed paired-pulse facilitation. Traces are scaled to the first EPSC amplitude for illustration. Scale bar: 50 ms. Paired-pulse ratios (PPR) were calculated as the ratio of the amplitude of the 2nd EPSC to the amplitude of the 1st EPSC. PPR did not differ between the groups (control: 1.2 ± 0.2 ; synaptophysin: 1.3 ± 0.2 ; synaptoPAC: 1.2 ± 0.2). **(C)** Traces showing the depletion of the readily releasable pool (RRP) of vesicles by a 6-s application of 500 mM sucrose. Scale bars: 0.5 nA, 1s. Groups did not differ in the size of their RRP, calculated as charge of the transient current evoked by the sucrose application (control: 1.3 ± 1.3 nC; synaptophysin: 1.5 ± 1.7 nC; synaptoPAC: 1.2 ± 0.8 nC). **(D)** Vesicular release probability (Pvr) of action potential-evoked EPSCs was not significantly different between the three groups. Pvr was calculated as ratio of the average EPSC charge to the RRP charge (control: $2.1 \pm 1.1\%$; synaptophysin: $1.6 \pm 0.7\%$; synaptoPAC: $1.8 \pm 0.8\%$). **(A-D)**: control: n = 24, N = 5; synaptophysin: n = 20, N = 5; synaptoPAC: n = 20, N = 3. **(E)** Representative EPSC traces evoked by 100 APs triggered at 10 Hz, normalized to the first EPSC amplitude. Scale bars: 0.5 (norm.), 1 s. Short-term plasticity was not markedly affected by overexpression of synaptophysin or synaptoPAC (control n = 20, N = 5; synaptophysin n = 17, N = 5; synaptoPAC n = 17, N = 3). Significance was determined using one-way ANOVA with Bonferroni *post hoc* test or Kruskal-Wallis test with Dunns *post hoc* test. Unclamped action potentials elicited by 1-ms current injections to 0 mV are blanked for clarity in traces shown in (A), (B) and (E).

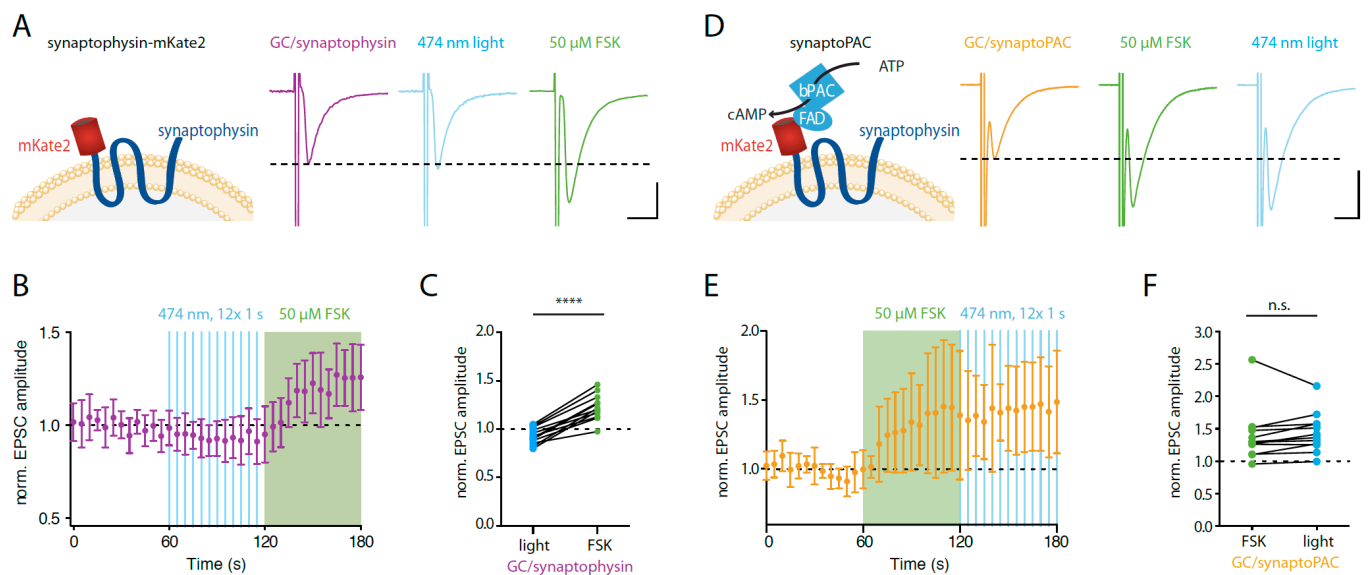


Figure S2: Control experiments demonstrating no effect of blue light on transmission in granule cells overexpressing synaptophysin, and a comparable potentiation of EPSCs by forskolin and light in synaptoPAC-expressing granule cells.

(A) Example traces from an autaptic granule cell expressing synaptophysin-mKate2 (illustrated on the left) exposed to blue light stimulation and subsequent forskolin application. Scale bars 2 nA, 10 ms.

(B) Time course of the normalized EPSC amplitudes recorded from synaptophysin-mKate2-expressing GCs during illumination with blue light and forskolin application. **(C)** Blue light pulses (470 nm, 70 mW·mm⁻², 12 x 1 s at 0.2 Hz) did not increase EPSC amplitudes, while application of 50 μM forskolin led to a potentiation of EPSCs in these cells (light: 0.92 ± 0.08 nA; FSK: 1.23 ± 0.13; n = 12; N = 4; paired t-test).

(D) Example traces from an autaptic granule cell expressing synaptoPAC exposed to forskolin and subsequent blue light stimulation. Traces are averages from six sweeps. Scale bars 0.5 nA, 10 ms. **(E)** Time course of the normalized EPSC amplitudes during forskolin application and light stimulation.

(F) Photostimulation did not further increase transmitter release in synaptoPAC-expressing granule cells already treated with forskolin (FSK: 1.40 ± 0.48 nA; light: 1.44 ± 0.48; n = 12; N = 2; paired t-test).

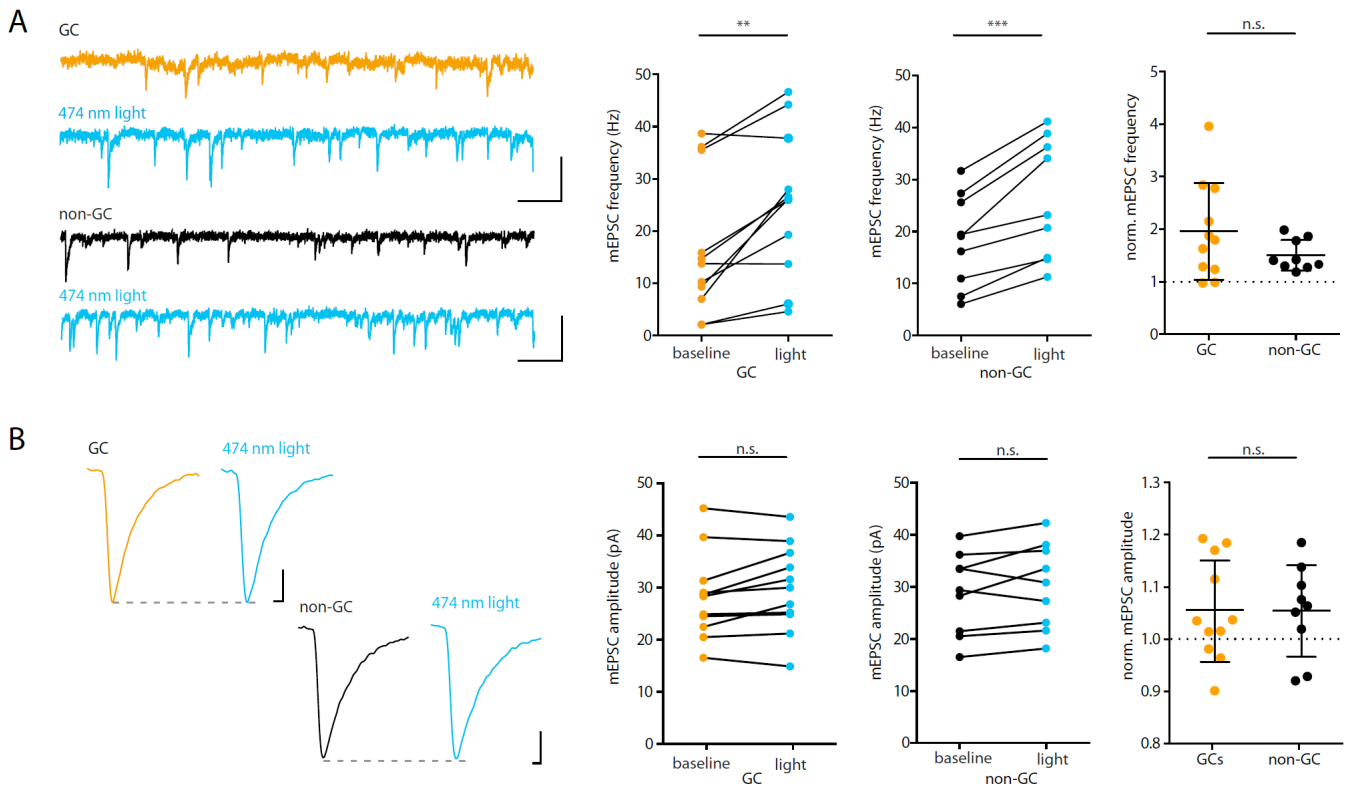


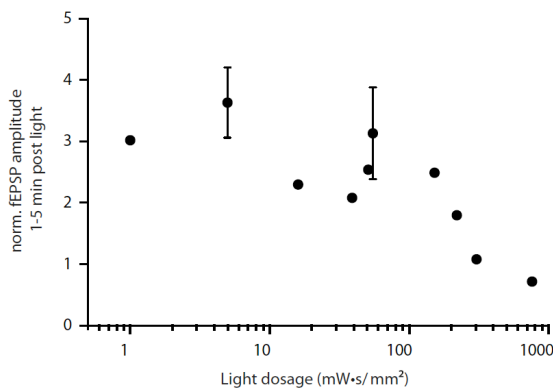
Figure S3. SynptoPAC activation increases the frequency but not the amplitude of mEPSCs.

(A) Example traces of mEPSCs of a GC (orange) and a non-GC (black) before and after light (blue). Scale bar: 50 pA, 100 ms. Light exposure increased the frequency of mEPSCs significantly compared to baseline both in GCs (baseline: 16.89 ± 13.6 Hz, light: 25.37 ± 14.0 Hz; $n = 11$, $N = 5$; $p = 0.002$, paired t-test) and in non-GCs (baseline: 18.2 ± 8.94 Hz, light: 26.2 ± 11.6 Hz; $n = 9$, $N = 4$; $p = 0.0003$, paired t-test). The change in mEPSC frequency in GCs was not significantly different from that in non-GCs (GC: 1.96 ± 0.92 , non-GC: 1.51 ± 0.2 ; $p = 0.13$, unpaired t-test). **(B)** Example traces of averaged mEPSCs of a GC (orange) and of a non-GC (black) before and after light (blue). Scale bars: 5 pA, 1 ms. SynptoPAC activation did not affect mEPSC amplitudes in GCs (baseline: 28.3 ± 8.27 pA, light: 29.8 ± 8.30 pA; $n = 11$, $N = 5$; $p = 0.082$, paired t-test) nor in non-GCs (baseline: 28.8 ± 7.85 pA, light: 30.2 ± 8.23 pA; $n = 9$, $N = 4$; $p = 0.148$, paired t-test). The mEPSC amplitudes normalized to baseline were not significantly different after light (GC: 1.06 ± 0.09 , non-GC: 1.05 ± 0.08 ; $p = 0.97$, unpaired t-test).

A

Light dosage (mW*s/mm ²)	Light intensity (mW/mm ²)	Pulse duration (s)	Number of pulses	Interstimulus interval (s)	norm. fEPSP ampl. 1-5 min post light	norm. fEPSP ampl. 20-30 min post light	Number of recordings
760	38	5	4	20	0.72	0.5	1
304	38	2	4	60	1.08	0.8	1
220	22	0.5	20	20	1.8	0.9	1
152	38	2	2	60	2.49	1.19	1
55	11	0.5	10	20	3.13 ± 0.75	1.26 ± 0.09	7
51	0.17	300	1	-	2.54	1.23	1
39	3.9	0.5	20	20	2.08	1.17	1
16.5	11	0.5	3	20	2.3	1	1
5.5	11	0.05	10	20	3.63 ± 0.57	1.25 ± 0.07	7
1.37	11	0.025	5	20	3.02	1.15	1

B



C

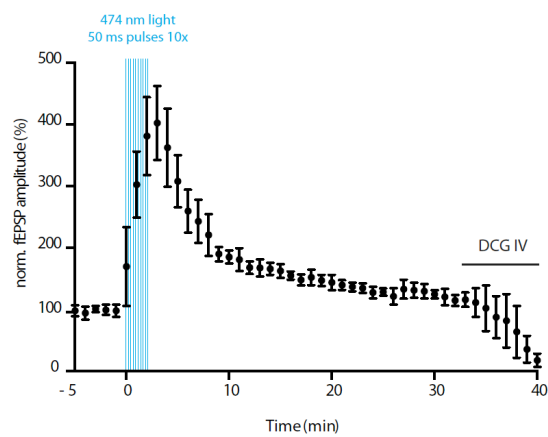


Figure S4: Light dosage titration for synaptoPAC activation in MF recordings in hippocampal slices.

(A) Overview table on different photostimulation protocols used for synaptoPAC activation in MF fEPSP recordings. High light dosages with long and high intensity light flashes had adverse effects, while low to medium light dosages induced comparable potentiation. **(B)** Diagram summarizing the relationship of light dosage and potentiation of fEPSPs after 1-5 minutes post light. **(C)** Summary graph of MF fEPSP recordings with 10 50-ms pulses of 470 nm light at 11 mW·mm⁻². This protocol results in 10x less light for the optical activation compared to Figure 3C (5.5 mW·s·mm⁻² vs. 55 mW·s·mm⁻² in Figure 3C), while yielding comparable potentiation directly after and 20-30 minutes post light stimulation (see Table in (A)). Data points shown are binned to 1 min.

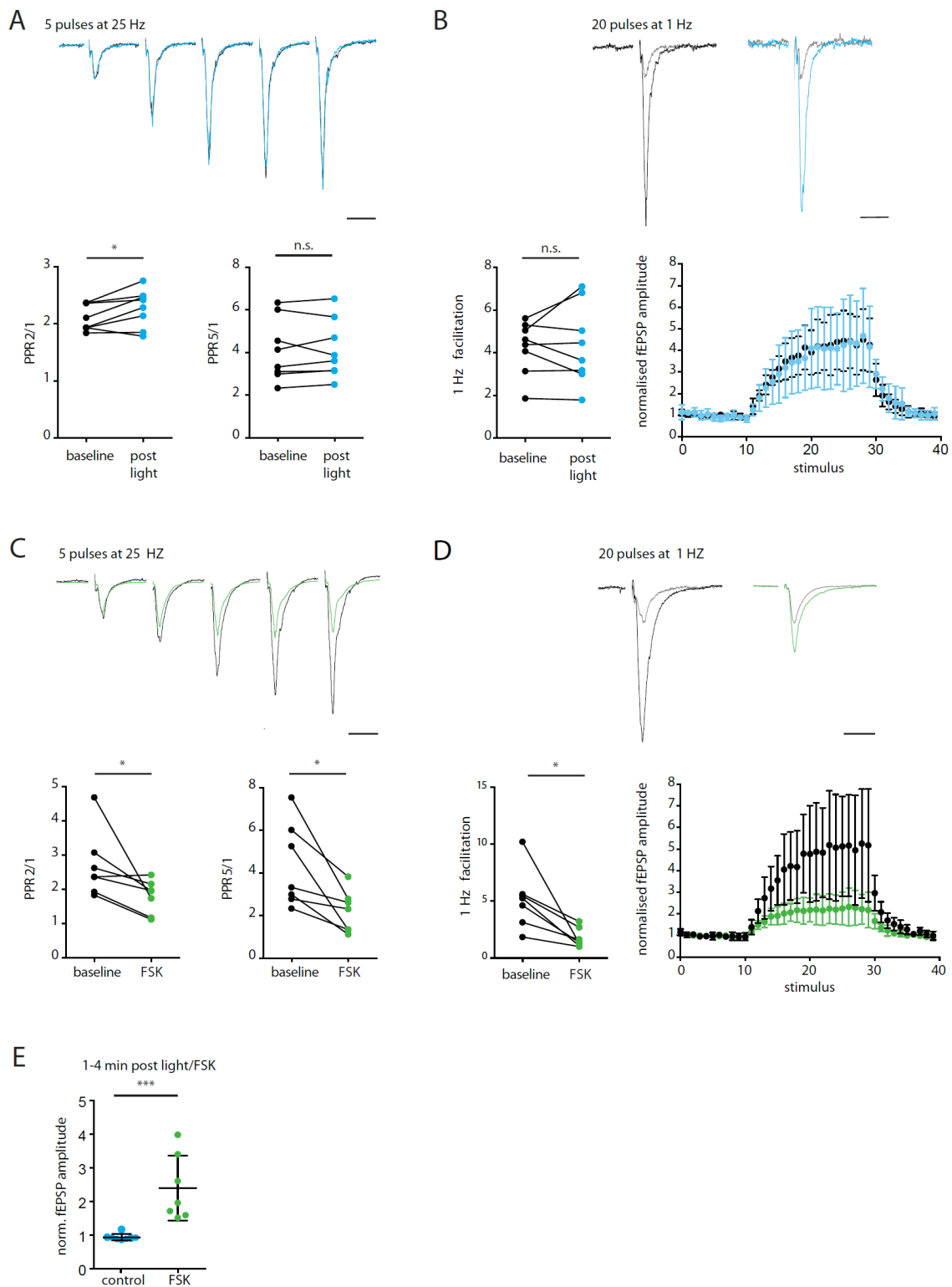


Figure S5: Facilitation of MF transmission is stable when repeatedly tested, but reduced by pharmacologically induced presynaptic potentiation.

MF short-term plasticity was tested in wild type mice not expressing synaptoPAC with the following protocol: during baseline MF were stimulated electrically with 5 pulses at 25 Hz and with 20 pulses at 1 Hz. Afterwards, 10 pulses of 470 nm light (500 ms, 11 mW·mm⁻², 0.2 Hz) or 50 μM forskolin for 10 min were applied. After light stimulation or forskolin application, the 25 Hz and 1 Hz stimulus trains were applied again after 5 and 10 min, respectively. **(A)** Representative traces of paired-pulse MF fEPSP before (black) and after light stimulation (blue), scaled to the amplitude of the first fEPSP. Scale bar: 20 ms. In the absence of synaptoPAC the paired-pulse ratio between the second and the first fEPSPs was

significantly increased after light stimulation (baseline: 2.11 ± 0.22 , post light: 2.27 ± 0.33 ; $n = 8$ slices, $N = 4$ mice; $p = 0.04$, paired t-test), in contrast to the significant decrease in recordings from synaptoPAC-expressing MFs. The paired-pulse ratio between the fifth and first fEPSPs was not different after light (baseline: 4.10 ± 1.46 , post light: 4.15 ± 1.38 ; $p = 0.73$, paired t-test). **(B)** Traces showing the first and last MF fEPSP evoked by a train of 20 stimuli applied at 1 Hz before (black) and after (blue) light illumination. Traces are normalized to the first fEPSP in baseline. Scale bar: 20 ms. 1 Hz facilitation did not change after light stimulation (baseline: 4.26 ± 1.24 , post light: 4.38 ± 1.87 ; $n = 8$ slices, $N = 4$ mice; $p = 0.73$, paired t-test). **(C)** Representative traces of paired pulse MF fEPSPs before (black) and after 50 μ M forskolin (green), scaled to the amplitude of the first fEPSP. Scale bar: 20 ms. Forskolin induced potentiation significantly decreased the paired-pulse ratio between the second and the first fEPSP ($n = 7$ slices, $N = 5$ mice; baseline: 2.70 ± 0.97 , post FSK: 1.79 ± 0.48 ; $p = 0.03$, Wilcoxon signed rank test), and the fifth and first fEPSPs (baseline: 4.32 ± 1.97 , post FSK: 2.19 ± 0.98 ; $p = 0.01$, Wilcoxon signed-rank test). **(D)** Traces showing the first and last MF fEPSP evoked by a train of 20 stimuli applied at 1 Hz before (black) and after (green) forskolin. Traces normalized to the first fEPSP in baseline. Scale bar: 20 ms. 1 Hz facilitation significantly decreased after forskolin induced potentiation ($n = 7$ slices, $N = 5$ mice; baseline: 5.18 ± 2.62 , post FSK: 1.76 ± 0.85 ; $p = 0.01$, Wilcoxon signed rank test). **(E)** Light (blue) and forskolin (green) effect on transmission at MF-CA3 synapses 1-4 min after the induction. Potentiation induced by forskolin ($n = 7$ slices, 5 mice; 2.40 ± 0.97) was significantly higher compared to the effect of light in animals not expressing synaptoPAC ($n = 8$ slices, $N = 4$ mice; 0.93 ± 0.97 ; $p = 0.0003$; Mann Whitney U test).

12. Curriculum Vitae

My curriculum vitae does not appear in the electronic version of my paper for reasons of data protection

13. Complete list of Publications

- Oldani, S.**, Moreno-Velasquez, L., Faiss, L., Stumpf, A., Rosenmund, C., Schmitz, D., & Rost, B. R. (2020). SynptoPAC, an optogenetic tool for induction of presynaptic plasticity. *Journal of neurochemistry*, 10.1111/jnc.15210.
- Nitzan, N., McKenzie, S., Beed, P., English, D. F., **Oldani, S.**, Tukker, J. J., Buzsáki, G., & Schmitz, D. (2020). Propagation of hippocampal ripples to the neocortex by way of a subiculum-retrosplenial pathway. *Nature communications*, 11(1), 1947.
- Brouwer, M., Farzana, F., Koopmans, F., Chen, N., Brunner, J. W., **Oldani, S.**, Li, K. W., van Weering, J. R., Smit, A. B., Toonen, R. F., & Verhage, M. (2019). SALM1 controls synapse development by promoting F-actin/PIP2-dependent Neurexin clustering. *The EMBO journal*, 38(17), e101289.
- Bernal Sierra, Y. A., Rost, B. R., Pofahl, M., Fernandes, A. M., Kopton, R. A., Moser, S., Holtkamp, D., Masala, N., Beed, P., Tukker, J. J., **Oldani, S.**, Bönigk, W., Kohl, P., Baier, H., Schneider-Warme, F., Hegemann, P., Beck, H., Seifert, R., & Schmitz, D. (2018). Potassium channel-based optogenetic silencing. *Nature communications*, 9(1), 4611.

14. Acknowledgments

First, I would like to thank my doctoral supervisor Dietmar Schmitz, who offered me the opportunity to be part of his great laboratory. He always kindly supported me with his scientific guidance and insights. He has distinguished himself as a leader who takes care not only of the remarkable scientific achievements, but also of the human aspect of his group, making sure that everyone in the laboratory feels comfortable and enjoy their time.

I would like to thank Benjamin Rost, who was my main mentor during this time and whose huge scientific knowledge I admire. For me he was an example of professionalism and resilience, skills that I hope I have learned from him (at least a little) and that will be useful to me in every field of my life. Thank you for always being present during the highs but especially during the lows of this long and amazing journey.

Sincere thanks to Lukas Faiss, Felicitas Brüntgens and Alexander Stumpf for being part of my project and Susanne Rieckmann, Anke Schönherr and Katia Czielsesky for their excellent technical assistance. I am grateful especially to Nikoalus Maier, Marta Orlando, Marcial Camacho-Perez and Claire Cooper for their feedbacks on this dissertation.

I would like to thank the NeuroCure and the SPP1926 for funding part of my PhD.

I feel extremely lucky to be part of the Schmitz lab and I am very grateful of being part a such an amazing group of people in which support, cooperation, fun and laughs were always present. Thank you so much to all the members, by far you have been the best part of my PhD.

Very special thanks goes to Laura Moreno-Velasquez and Roberto de Filippo, who were for me not only friends and lab mates, but also my “Berlin family”.

Thanks you also to Alessandro, Simona, Michelle, Stefanie and Andrea: without your companionship, life outside the lab wouldn't have been possible.

Finally thanks to my family: my mother, my father, Marco, Leonardo, Lilli and Liebe, who represents my my lighthouse, my safe harbour, the source of unconditional love and my roots. All the achievements that I might reach in my life are also yours. Grazie di cuore a tutti voi.